NBS

Technical Note 279

FLUX AVERAGING DEVICES FOR THE INFRARED

S. THOMAS DUNN

U. S. DEPARTMENT OF COMMERCE
NATIONAL BUREAU OF STANDARDS

THE NATIONAL BUREAU OF STANDARDS

The National Bureau of Standards is a principal focal point in the Federal Government for assuring maximum application of the physical and engineering sciences to the advancement of technology in industry and commerce. Its responsibilities include development and maintenance of the national standards of measurement, and the provisions of means for making measurements consistent with those standards; determination of physical constants and properties of materials; development of methods for testing materials, mechanisms, and structures, and making such tests as may be necessary, particularly for government agencies; cooperation in the establishment of standard practices for incorporation in codes and specifications; advisory service to government agencies on scientific and technical problems; invention and development of devices to serve special needs of the Government; assistance to industry, business, and consumers in the development and acceptance of commercial standards and simplified trade practice recommendations; administration of programs in cooperation with United States business groups and standards organizations for the development of international standards of practice; and maintenance of a clearinghouse for the collection and dissemination of scientific, technical, and engineering information. The scope of the Bureau's activities is suggested in the following listing of its three Institutes and their organizational units.

Institute for Basic Standards. Applied Mathematics. Electricity. Metrology. Mechanics. Heat. Atomic Physics. Physical Chemistry. Laboratory Astrophysics.* Radiation Physics. Radio Standards Laboratory:* Radio Standards Physics; Radio Standards Engineering. Office of Standard Reference Data.

Institute for Materials Research. Analytical Chemistry. Polymers. Metallurgy. Inorganic Materials. Reactor Radiations. Cryogenics.* Materials Evaluation Laboratory. Office of Standard Reference Materials.

Institute for Applied Technology. Building Research. Information Technology. Performance Test Development. Electronic Instrumentation. Textile and Apparel Technology Center. Technical Analysis. Office of Weights and Measures. Office of Engineering Standards. Office of Invention and Innovation. Office of Technical Resources. Clearinghouse for Federal Scientific and Technical Information.**

---

*Located at Boulder, Colorado, 80301.
**Located at 5285 Port Royal Road, Springfield, Virginia, 22171.

NATIONAL BUREAU OF STANDARDS

Technical Note 279

ISSUED DECEMBER 9, 1965

FLUX AVERAGING DEVICES FOR THE INFRARED

S. Thomas Dunn

NEXT

NBS Technical Notes are designed to supplement the Bureau's regular publications program. They provide a means for making available scientific data that are of transient or limited interest. Technical Notes may be listed or referred to in the open literature.

For sale by the Superintendent of Documents, Government Printing Office
Washington, D.C., 20402 - Price 30 cents

CONTENTS

ILLUSTRATIONS

FIGURE

FLUX AVERAGING DEVICES FOR THE INFRARED*

by

S. Thomas Dunn†
National Bureau of Standards
Washington, D. C.

ABSTRACT

The spatial and angular sensitivity of infrared detectors recently has been investigated (1, 2). In order to eliminate this effect and obtain accurate measurements in the infrared, it is necessary to distribute the flux as uniformly as possible over the entire sensitive area of the detector. A solution to this problem is presented in the form of several averaging devices developed at the National Bureau of Standards. Among the devices investigated are roughened NaCl windows, diffusing light ducts, and spheres with different coatings. Each device was subjected to a series of tests to establish its averaging capability and useful wavelength range. Results of these tests indicate that the use of a small sulfur-coated hollow sphere over the detector increased the accuracy of most types of infrared reflectance measurements and, at the same time, decreased the requirement for precise optical alignment of the detector in the wavelength range of 1.5 to 8 microns. The use of the sulfur-coated sphere over a thermopile extends the usefulness of the multiple-reflection specular reflectometer to about 10 microns. (Key Words: Detector, Averaging Device, Spatial Sensitivity, Angular Sensitivity, Sulfur, and Integrating Sphere).

*The work described in this paper was done under NASA Contract No. R-09-022-032.

†Member of Photometry and Colorimetry Section, Metrology Division, Institute for Basic Standards.

INTRODUCTION

From the turn of the century, large area thermopiles have been used as infrared radiation detectors for large area beams. It is astounding that for all this time the general practice has been to use these detectors as though they were spatially insensitive.1/

Only recently have experimental measurements been reported that confirm the fallacy of this assumption (1). The spatial sensitivity for a ten-junction thermopile is shown in figures 1 and 2. Appendix A describes the thermopile concerned and the method of measurement.

Spatial sensitivity is not a unique property of thermopiles. The spatial sensitivity of the Golay cell (fig. 3 and 4), the lead sulfide cell (1), and the photomultiplier tube (1) have all been illustrated. M. Finkel 2/ has found the large area InSb detector to be similarly spatially sensitive. Thus, it is apparent that if a large area detector is to be used to accurately compare a small area beam with a large area beam (2), or to compare two beams of similar size (but smaller than the detector), it will be necessary to use some flux averaging device. Figures 6 and 7 illustrate that the angular sensitivity 3/ of a ten-junction thermopile (appendix A) is such that to accurately compare beams incident on the detector from different directions, with different solid angles, or with marginal rays exceeding an angle of 25° from the normal to the sensitive area of the detector, it will be necessary to use an averaging device with the detector. Furthermore, the comparison of beams or images whose irradiance varies with position will require the use of an averaging device over the detector (3). In general, problems of angular and spatial sensitivity occur in all focusing optical systems. END.

FLUX AVERAGING DEVICES

The data obtained on the spatial and angular sensitivity of detectors indicate that a flux-averaging device would be required for use with any of the available large-area infrared detectors. The function of such a device is to distribute the available flux uniformly over the sensitive area of the detector, regardless of image size, shape, or intensity distribution. Any averaging device will, of course, reduce the efficiency of a detector system, because some of the incident flux is absorbed by the diffuser, and some is scattered away from the sensitive area and is lost. In general, the losses in a diffuser tend to increase with an increase in its effectiveness as a diffuser.

The literature provides several references to flux-averaging devices. One is the work of Bennett and Koehler (4), who used a small integrating sphere to average the incident radiation over a photomultiplier detector. Another is the work of Ronzhin (5), who tried light ducts and integrating spheres to average radiation over the sensitive area of a photomultiplier. However, these references offer solutions only in the ultraviolet, visible, and near infrared portions of the spectrum, where good integrating sphere coatings are available. In the infrared, no one has yet shown that satisfactory integrating sphere coatings exist for use beyond 4 microns. Reference (1) also illustrates the use of several similar averaging devices.

1/ Spatial sensitivity is defined as variation in response of the detector with change in the irradiated portion of the sensitive area.

2/ Photometry and Colorimetry Section, Metrology Division, Institute for Basic Standards, National Bureau of Standards.

3/ Angular sensitivity is defined as the variation in response of the detector with angle of incidence (with respect to the sensitivity area of the detector) of the measured flux.

Three different types of diffusing devices were investigated. They are listed in estimated order of increasing degree of diffusion as: 1) a diffusing screen placed directly over the detector, 2) a light duct with diffusing walls or a diffusing surface in the system, and 3) an averaging sphere[1/] coated with a material having high reflectance in the infrared and sufficient diffusion to permit it to be used as an averaging device.

To establish the usefulness of the various averaging devices, three tests were devised as follow:

1. Test A - Spatial Sensitivity: This test was designed to illustrate the required precision of incident image placement for comparing beams of nearly the same image area. The general optical system for this and the following tests is shown schematically in figure 5. A 6-inch-diameter spherical mirror of 49-inch radius was used to form an image of the monochromatic source on the entrance port of the averaging device. The averaging device, with the detector, was mounted in a milling head, so that it could be moved 8 inches in the x and y directions, and rotated 360 in the x-y plane. The x direction is aligned with the optical axis.

In the spatial sensitivity test, the averaging device was mounted at the center of the milling head, with its plane of entrance perpendicular to the incident beam from the spherical mirror. The entrance port of the device was then moved across the incident beam (the size of this beam was 3 mm by 3 mm) and the detector response was recorded as a function of beam position.

2. Test B - Area Sensitivity: This test was designed to evaluate the variation in detection response with the size of the irradiated area on the entrance to the averaging device, when the total flux is held constant. The detector and averaging device were mounted on the milling head (figure 5) with the axial ray of the incident beam (3 mm by 3 mm) centered on and normal to the entrance port of the averaging device. The port was moved along the axial ray of the incident beam, and the detector response was recorded as a function of the entrance port position. Since the incident beam is diverging from an image, the size of the irradiated area could be varied from a minimum when the beam was imaged on the entrance port, to a maximum when the marginal rays fell just inside the port.

3. Test C - Angular Sensitivity: In this test, the averaging device was placed on the milling head and the image from the 49-inch radius of curvature mirror was placed on the entrance to the averaging device. The output of the detector was recorded as a function of incident angle as the milling head was rotated (appendix A). The recorded data were then normalized to a specified direction.

When results of any one of the three tests indicated a particular averaging device to be unsuitable, no further tests were made.

DIFFUSING SCREENS

The first device tested was a roughened sodium chloride window. The data in figure 8 were obtained in the same manner as those reported for figures 1, 2, 3, and 4, except that a diffusing screen holder is now placed against the detector entrance window. Diffusing screen No. 2 was 5 mm thick, and one surface had been ground with a 9.5-micron abrasive.

1/ A distinction is made between an integrating and an averaging sphere. In the case of the averaging sphere, the main requirement is that the distribution and fraction of the incident flux on the detector must be independent of the area of the sphere wall irradiated for a certain specified area on the sphere, while the integrating sphere assumes uniform diffusion of flux over the entire sphere wall (with the exception of the directly irradiated portion).

Screen No. 3 was 2.5 mm thick, and one surface had been ground with a 50-micron abrasive.

In figure 8, it can be seen that diffusing screen No. 3 had only a slight effect in smoothing out the peaks, but diffusing screen No. 2 was more effective, and produced a relatively uniform response across the sensitive area of the detector in both the a-c and d-c scans.

It is apparent from the reduced spatial sensitivity shown in figure 8, (compared to figures 1 and 2) that the roughened window would be useful for reasonably accurate comparison of small beams[1/] (with respect to the detector area) that were accurately positioned in the center of the detector sensing area. This device would not be good for use in measuring beams of about the same size as the detector area, since much of the flux would be scattered away from the sensitive area of the detector, and possibly, in some thermopiles onto the cold junctions, thus yielding false indications.

DIFFUSING ELBOWS

The second device tested was a diffusing elbow, shown in figure 9. This elbow greatly reduced the spatial sensitivity when the flux was incident on one end of the elbow, and the detector was placed at the other end. However, figure 10 indicates that the elbow-detector combination had high angular sensitivity in the plane of incidence across the diffusing surfaces, while figure 11 shows relatively little angular sensitivity in the plane of incidence perpendicular to the mirror surfaces. Figure 12 is an improved design, in which the walls are all mirrors, except for the diffusing 45° surface used to reflect the incoming radiation toward the detector. The diffusely reflecting surface used with this device consists of a series of spherical depressions in aluminum, each of 1/16-inch radius, spaced 0.088 inch apart in a hexagonal, close pack, array. A goniophotometric reflectance curve for this surface for white light incident at 45° is shown in figure 13. This surface has since been liquid honed, and then gold plated. The liquid honing gives a diffusing surface of small roughness, which, in combination with the large roughness of the spherical depressions, should reduce the height of the specular peak at 45° in figure 13.

Figure 14 illustrates the spatial sensitivity (test A) of this elbow as a small image is traversed across the entrance port. The signal from a small area beam can be reproduced by positioning the elbow to yield a maximum detector response. Figure 15 represents the area sensitivity test for the case when, for A/(A minimum) = 1, the elbow is moved until a maximum reading is obtained (figure 14) and then the area sensitivity of the elbow is measured (test B). Figure 15 indicates that the decrease in signal for the large areas can be calibrated; that is, the device senses the largest area signal about 20 percent lower than the smallest area signal of the same flux content. Thus, careful calibration and measuring techniques would allow use of a device of this nature for reducing spatial sensitivity for large area detectors.

However, even with careful calibration of this device, errors of up to 5 percent may be present in comparisons between beams of flux of different cross-sectional areas.

AVERAGING SPHERES

Since none of the devices described so far provided the desired spatial insensitivity, an averaging sphere was tried.

Preliminary results, using a 2-inch-diameter sphere mounted over the detector, with a 3M white velvet diffusing paint coating, indicated that this approach seemed feasible, at

---

1/ Neglecting the case where roughened windows are used over detectors to enable them to view an entire sphere.

least at short wavelengths where known diffusers are available (6). It is known from the theory of integrating spheres (7) that for sphere efficiency to be high, it is necessary for 1) the wall reflectance to be close to unity, 2) the diameter of the sphere to be a minimum, and 3) the area of the entrance and exit ports to be a minimum. In addition, the detector should also view the entire sphere. Further, it is important that the sphere wall be a diffusing surface if a constant irradiance across the detector port is to be attained.

High sphere efficiency is required in this application, because the amount of flux available for measurement in the infrared is near the lower limit of the useful range of the available detectors, particularly at the longer wavelengths. Certain white paints, MgO, and $BaSO_4$ are good sphere coatings in the visible and near infrared, but they have low reflectance beyond 4 or 5 microns and are not suitable for use at longer wavelengths. Birkebak (8) showed that sulfur is both a good diffuser and reflector at 2 microns and 4 microns, and assumed that it is usable to 10 microns. However, he did not mention the specific form of sulfur that was used for his measurements, or his method of applying it to the sphere wall. Kronstein, et al (9) reported that mu sulfur and flowers of sulfur are good reflectors out to 15 microns, and gave spectral reflectance curves, but did not use sulfur as a sphere coating. Agnew and McQuistan (10) showed that sulfur is a diffuse reflector to the flux from a Globar with wavelengths shorter than and longer than 4 microns. Data on the reflectance of mu sulfur is given in figure 16 (2).

Polished metals have high reflectance at all wavelengths from the near infrared to the far infrared, but they are not suitable for use in integrating spheres, since they reflect specularly. Roughening the surface of a polished metal, however, will on reflection diffuse the incident beam. Hence, it may be possible to produce a usable sphere coating by first contouring a metal surface and then applying a vacuum-deposited metal coating to increase the surface reflectance. In the present work, two general types of surfaces were considered for use as an averaging sphere coating in the infrared: 1) a roughened gold-plated surface, and 2) a sulfur coating.

Many spheres were built and coated. The following is a partial list of those tested:

1. A 4-inch-diameter aluminum sphere coated with smoked MgO. The entrance and detector port areas were 0.188 $in.^2$ and 0.875 $in.^2$, respectively.

2. A 2-inch-diameter sphere roughened by "roto-blasting" with spherical glass shots.[1/] The sphere was then vapor plated with an opaque coating of gold. Entrance and exit port areas for all the 2-inch spheres utilized in this paper are 0.444 $in.^2$, and 0.515 $in.^2$, respectively.

3. A 2-inch-diameter sphere coated with sulfur[2/]. The sulfur was handpressed onto a roughened sphere wall.

4. The roughened, gold-plated sphere wall of sphere 2., above, was overcoated with a very thin coat of sulfur. The sulfur was suspended in alcohol and sprayed with an ordinary paint sprayer.

1/ The Roto-Blast process is a trade name used by Pangborn Corp. to describe the blasting of surfaces, in this case with spherical shot. Both glass and steel spherical shot are available from this company. The roughened spheres used in this investigation were Roto-Blasted by Mr. Mann of Pangborn Corp., Hagerstown, Maryland.

2/ The sulfur used in this investigation was Crystex brand sulfur and was supplied by Mr. A. Blackwell, Manager, Technical Service Department, Stauffer Chemical Company, 380 Madison Avenue, New York, N. Y. The analysis given by the supplier is 99.5% Elemental Sulfur, 90% mu (insoluble) sulfur, 0.10% ash, and the acidity is 0.05%. Mu (insoluble) sulfur comprises 90% of elemental sulfur.

5. A 2-inch-diameter sphere was coated with a 1/8-inch-thick coating of sulfur, which had been sprayed from a suspension in alcohol.

6. A 2-inch-diameter sphere was coated with a 1/8-inch-thick coating of sulfur, which was sprayed from a suspension in benzene.

Appendix B describes the methods of coating or preparing the sphere wall.

Test B: Area Sensitivity[1/]

In order to establish the ability of the averaging sphere-detector combination to compare beams of flux of various sizes, the previously described area sensitivity test was performed. See figure 5 for detector viewing configuration.

The measured sphere position was experimentally correlated to the area of sphere wall irradiated by the incident beam, and each area was divided by the cross-sectional area of the beam at the focal plane of the spherical mirror to obtain the area ratio for each position. The detector response at each position was divided by the response at the position where the flux was focused on the sphere wall, to obtain the response ratio R/R_o. Response ratio was then plotted as a function of area ratio to obtain the curves shown in figures 17, 19, and 20.

This test simulates the conditions that exist when the detector is used to compare beams of flux of small and large areas. The maximum area ratio attainable with the described experimental arrangement was 12.25 to 1 for the 2-inch-diameter sphere, and about 2.36 to 1 for the 4-inch-diameter sphere.

The area sensitivity test was applied to all the spheres considered for use as averaging devices. The data at the top of figure 17 represent the results for MgO at 1.5 microns, where it is a known good diffuser. R/R_o varied by 0.8 percent for an area ratio 2.36 to 1. Since the sphere was 4 in. in diameter, the optics of the test system limited the area changes of the image on the sphere wall to a smaller ratio than for the 2-inch-diameter spheres used for the other materials in the test. The results indicate that the sphere does indeed reduce the area sensitivity of the detector. However, MgO is not suitable for general use as a coating in the infrared.

The second curve in figure 17 represents the results for a roughened sphere, which had been vapor-plated with gold; the roughness of the sphere wall was of the order of 25 μ-in. rms. The change in R/R_o was 2 percent, indicating poorer diffuseness than for the MgO. Further, the efficiency of this sphere is almost identical to that of the other spheres tested, despite the very high reflectance of gold. In this design there is a large specular component of flux that passes out the entrance port of the sphere on the first reflection from the sphere wall. Thus, to increase the efficiency of a sphere of this design, the specular component of the first reflection must be kept in the sphere; on the other hand, it must be kept away from the detector's sensitive area, since slight variations in image placement would yield large changes in detector response.

Figure 17 shows the data for Crystex brand sulfur, which was hand pressed onto the sphere wall. These data have a spread of 0.6 percent in R/R_o and illustrate the usefulness of sulfur for an averaging sphere coating; however, the application technique yielded a surface that was extremely fragile and whose reflectance probably varied significantly from point to point over the sphere wall. Thus, other methods were tried to obtain a more uniform and mechanically durable surface. First, the gold sphere referred to above was coated with a very thin layer of Crystex sulfur. The sulfur was suspended in alcohol and applied with a paint spray gun. The results of the area sensitivity test indicate a variation in R/R_o of 1.1 percent. Further, the efficiency of this sphere was nearly the same as that of

---

1/ The order of the tests on this device has been inverted for sake of clarity.

the hand-pressed sulfur sphere. Since the efficiency was the same, and R/R_o showed a greater change than that of the hand-pressed sulfur sphere, it was decided to try spraying an optically opaque 1/8-inch-thick coat of sulfur. This sphere exhibited the same change in R/R_o as the hand-pressed sphere and the coating was less fragile.

To further reduce changes in R/R_o, two different methods of shielding the detector viewing area were tried. Shielding is useful because the detector does not view the entire sphere equally well, as is illustrated by its angular sensitivity in figures 6 and 7. The primary function of a shield is to prevent the detector from viewing the directly irradiated area on the sphere wall for all image configurations. The first shield, which is illustrated in figure 18a, was a 0.15-inch-thick disk placed over the detector with a 1/2-inch-diameter hole centered over the detector sensing area. The sides of this hole were coated with Parson's black paint, and thus restricted the detector's field of view. The results are presented in the second to last graph in figure 17, and indicate an over-all range in R/R_o of 0.6 percent for an area ratio spread twice as large as for the hand-pressed sphere. The second shield tested is shown in figure 18b. This shield was tried because it yields a higher detector efficiency, since it only restricts the detector viewing field in the direction of the image on the sphere wall. The shield was constructed of 0.005-inch-thick polished platinum. The data for this sphere are plotted in the last graph of figure 17 and show a 0.4 percent variation in R/R_o. Thus, these tests indicate that either of the spheres with detector shields are usable at 2.4 microns.

These two spheres were tested at other wavelengths in the range 1.5μ to 7.0μ. The results for the platinum shield (shield 2) are given in figure 18. Note that the scale of the graphs for the longer wavelengths is smaller. This figure shows that at the longer wavelengths, where sulfur's reflectance is lower, R/R_o decreases with an increase in A/(Amin.) as much as 2.8 percent. This could be caused 1) by the incident flux becoming trapped between the platinum shield and the sulfur wall (this would be more pronounced at the longer wavelengths, because the reflectance of the sulfur wall is lower), or 2) by atmospheric absorption in the increased path length due to water and CO_2 in the atmosphere. Such atmospheric absorption is not probable, since the wavelengths used were between the absorption bands (the results in figure 20 for the sphere with the circular disk shield substantiate this conclusion).

Since the change in R/R_o for the sphere with the platinum shield was quite large at the longer wavelengths, the sphere configuration using the circular disk was also tested at these wavelengths.[1/] The results of the tests for variation of response with image size are given in figure 20. These results show an increase in detector sensitivity with image size, indicating that part of the flux is still reaching the detector on the first reflection for large images. However, the change in R/R_o is limited to 0.9 percent for the longest wavelength. The reason that the change of R/R_o varies with wavelength is that the reflectance of sulfur varies with wavelength. With low sphere wall reflectance (i.e., long wavelengths for sulfur), the flux from the first reflection is a major portion of the flux in the sphere; and if the detector views even a very small amount of this flux (which is the case for large images on the sphere wall), there is a significant increase in detector response (2). This error can be eliminated by increasing the thickness of the shield shown in figure 18; however, this will reduce the efficiency of the sphere, which is intolerable, because the system is already energy limited in the 7-10 micron region when a thermopile detector is used.

The conclusions from this series of test are that a sulfur sphere with the circular disk shield provides a better averaging device for signals of different image sizes. It should be noted that sulfur has several absorption bands in this range, which may be

---

1/ Since the previous tests, this sphere had been recoated with sulfur sprayed from a benzene suspension, which yielded a coating that was more stable mechanically than that sprayed from an alcohol suspension.

detrimental for certain applications depending on high spectral resolutions.

Test A: Spatial Sensitivity

This test was designed to illustrate the required precision of incident image placement for comparing signals of nearly equal image area. The sphere entrance port was traversed across the incident beam, which was focused on the entrance port and had a 3 mm by 3 mm area.

The results for the sulfur sphere with the internal platinum shield are presented in figure 21. The data are arbitrarily normalized to one of the central readings and plotted as function of position on the entrance port as measured from one edge. These data show variations exceeding 2 percent at the longer wavelengths.

Results for the sphere with the circular disk shield show variations of less than 0.4 percent for the wavelengths below 5.5 microns, and variations of about 0.8 percent for the longer wavelengths (figure 22). This again illustrates the effect of the first reflected flux, since at the long wavelengths, where the reflectance of sulfur is lower, the detector signal is higher for images between positions 0.4 and 0.6 on the entrance port of the sphere, which is where more of the once reflected flux could reach the detector (left-hand side of sphere opening in figure 18).

The results of these tests indicate that for short wavelengths the position of the incident flux on the entrance port is not very critical, while at longer wavelengths more care must be taken in positioning the incident beam.

Test C: Angular Sensitivity

The general optical system for the angular sensitivity test is shown schematically in figure 5. In this test, the sphere was positioned with its entrance port at the center of rotation of the milling head, and the incident beam was centered on the entrance port. The sphere was ten rotated, and the response of the detector was recorded as a function of the angular position of the sphere measured as the angle between the axial ray of the incident beam and the normal to the sphere entrance port.

If a perfect integrating sphere were tested in this way, and the detector viewed only a portion of the sphere wall, as illustrated in figure 23, then the signal from the detector would change as the irradiated spot moves around the sphere, by an amount proportional to the difference in radiance of areas on the sphere wall that are and are not directly irradiated by the incident flux. If the area irradiated by the incident flux is not viewed by the detector, no flux that has been reflected only once will be received by the detector. Thus, for a surface that approaches an ideal integrating sphere coating, the curve of response as a function of angle should show two ranges of nearly constant response with a smooth monotonic transition between the two ranges. The lower range would represent those angles at which the detector views none of the irradiated area, and the higher level would represent those angles at which it views the entire irradiated area, and the transition would represent those angles at which the detector views an increasing fraction of the irradiated area. Reference 2 gives equation (1) as the quantitative description of this change for the perfect diffuser as the ratio (R) of the reading when the detector does not view the directly irradiated area to the reading when it views the directly irradiated area.

$$R = \frac{1}{1 + \dfrac{(f_2/f_1)[A_S - \rho_S A_{SH}]A_S}{\rho_S (A_{SH})(A_{DV} - A_{H2})}} \qquad (1)$$

where A_S is the total area of the sphere ($A_S = 4\pi R^2$), $A_{SH} = A_S - A_{H1} - A_{H2}$ (A_{H1} and A_{H2} are the areas of the exit and entrance ports, respectively), A_{DV} is the area of the sphere fully viewed by the detector, $(A_{DV} - A_{H2})/A_S$ is the proportion of the twice-reflected flux in the area viewed by the detector, f_1 is the diffuse configuration factor from area $(A_{DV} - A_{H2})$ to the sensing element of the detector, f_2 is the configuration factor from the

area irradiated by the beam to the detector sensing element, and P_s is the reflectance of the sphere wall.

Figure 24 shows results obtained with the gold-plated S-460 shot, 2-in.-diameter sphere, at wavelengths of 2.2, 5, and 8 microns. In this case, the detector port is in the plane of incidence, and is diametrically opposite the entrance port. The curves indicate that there is a large specular component of the reflected flux reaching the detector when the angle is about 50°, and that the reflectance characteristics do not change appreciably with wavelength. The S-460 shot surface has a roughness of about 150μ in. rms; hence, no effect of wavelength would be expected in this range. This figure illustrates that the position of the incident beam on the inside of the sphere is quite critical and indicates the necessity of keeping the first reflection away from the detector port in a sphere with imperfectly diffuse walls.1/

The sulfur sphere coating outlined earlier was tested in this manner. Figure 25 illustrates the results for sulfur at 1.5, 2.2, 5.0, and 10.0 microns. Each of these curves illustrates two flat regions with a smooth montonic transition between the regions. These results gave a qualitative indication of the utility of sulfur surface as an averaging sphere coating. Further, the flatness of the flat regions suggests that the placement of a beam inside the sphere is not as critical as with the roughened metal sphere walls.

In addition, the ratios of the heights of the flat portions of these curves (figure 25) agree with the trends indicated in equation (1). However, the ratios calculated from the data in figure 25 were consistently lower by a factor of 2-3 than would be predicted by theory [equation (1)]. Apparently, the experimental set-up did not entirely fit the theoretical model. Several possible sources of error are:

1. The flux from the irradiated area when it is not directly viewed by the detector (i.e., when the incident flux is in area c-d in figure 23) could reach the detector by paths other than by being multiply reflected from the d-a-b-c area viewed by the detector, by (a) hitting the lip of the detector port and being diffused to the detector by scratches on the CsBr window. The net effect would be to increase the height of the low flat portion of the curves in figure 25.

2. The radiation in the a-b area of figure 23 is incident at near grazing angles, where even the best diffusers tend to become somewhat specular. Thus, some flux is reflected around the sphere wall into the area c-d, which is not viewed by the detector, instead of being diffusely reflected to the detector. The net effect would be to reduce the height of the high flat portion of the curves in figure 25.

3. Using the wrong value for A_{DV} in equation (1).

4. Using the wrong value for the reflectance of the sulfur coating.

5. Improper evaluation of f_1 and f_2.

The first two effects are largely responsible for the low ratio of the two signals, as compared to the ratio computed from equation (1).

From the results established in this section, it can be stated that the use of an averaging sphere can be extended at least to 7 microns by use of sulfur as a sphere wall coating. Further, the inherent advantage of this approach is the ability to accept images of varying size by use of a large entrance port and to measure accurately the total flux contained in various incident beams. The major disadvantage is the reduction (by about 90 percent) of the flux that reaches the detector.

1/ In addition, this test illustrates that roughened surfaces do not and cannot follow the integrating sphere model in any respect; thus, it does not appear promising as a true integrating sphere coating, as has been proposed by several investigators.

SUMMARY

The summary of this work is presented in four parts: (a) the sulfur-coated averaging sphere, (b) suggested improvements to the gold-roughened sphere, (c) other averaging devices or techniques, and (d) present use of averaging spheres in the infrared.

(a) The Sulfur-Coated Averaging Sphere. The data presented indicate that, of the diffusers or averaging devices tested, the sulfur-coated sphere (with a shield restricting the viewing field of the detector) provides highest accuracy in comparing beams of different geometry. Additional advantages accrued through the use of an averaging sphere are 1) practically any detector geometry can be used to view the sphere, regardless of sensitive area or type, 2) the use of an averaging sphere greatly reduces the problem of optical alignment, since minor variations in beam placement do not affect the signal output of the detector, and 3) the careful use of the averaging sphere with the detector will provide the capability to measure flux very accurately [more accurately than can be read from the commonly used 10-inch strip chart recorder (additional accuracy can be obtained by use of a digital readout)].

The major disadvantages of the averaging sphere are the low efficiency of the sphere (the order of 10% for those spheres tested) and the fact that the sphere reflects flux back out the opening. The efficiency of the sulfur-coated averaging sphere decreases significantly at wavelengths beyond about 10 microns, because of the decrease in wall reflectance. However, the tests on the sulfur sphere reported in this paper, combined with the data in references 2 and 8, indicate that sulfur is usable as an averaging sphere coating out to at least 10 microns.

(b) Suggested Improvements to the Gold-Roughened Sphere. Since a prime reason that the sulfur-coated sphere cannot be used beyond 10 microns is sulfur's low reflectance between 10 and 15 microns (9), it is desirable to improve the performance of the gold-roughened sphere. The following two methods are proposed to accomplish this: 1) design the sphere so that the first three specular reflections of the flux do not strike the detector or entrance port of the sphere (especially, keep them away from the detector viewing port), or 2) place an optically opaque coating of sulfur (or some other body scatterer for wavelengths longer than 20 microns, such as ground-up CsBr) over the directly irradiated area of the sphere to diffuse the flux on the first reflection. For best results, care should be taken to prevent the detector from viewing any of the diffusing material.

(c) Other Averaging Devices or Techniques. Several methods of averaging various beams of flux that were not experimentally studied are 1) the use of lenses over the detector, 2) the use of condensing cones (which have inherent angular and spatial sensitivity), 3) the viewing of diffusing blocks which have high spatial sensitivity and low angular sensitivity, and 4) the use of statistical methods to compare various detector signals by traversing the sensitive area of the detector for each beam and cross-correlating the resulting sensitivity curves. This last approach is being investigated at this time by Mitchell Finkel.[1/]

(d) Present Use of the Averaging Sphere in the Infrared. The author (2) has successfully used the sulfur-coated averaging sphere to improve the accuracy of the elipsoidal mirror reflectometer and to construct a simple, but accurate, multiple-reflection, infrared, specular reflectometer. In both cases, an increased accuracy accompanied a decrease in the required precision of optical alignment. Reference (3) illustrates the use of the gold-roughened sphere to average flux from various sources over the entrance slits to a monochromator.

The author would like to express his appreciation to John A. Wiebelt[2/] and Joseph C. Richmond[1/] for helpful suggestions, and to John T. Perone, Jr.[1/], for taking much of the experimental data.

1/ Photometry & Colorimetry Section, National Bureau of Standards.

2/ Associate Professor of Mechanical Engineering at Oklahoma State University.

APPENDIX A

MEASUREMENT OF DETECTOR SPATIAL AND ANGULAR SENSITIVITY

Spatial Sensitivity

The spatial sensitivity (figures 1 through 4) was measured by W. Schneider, Photometry and Colorimetry Section, National Bureau of Standards (1).

The thermopile was mounted on an automatically driven micrometer head that could move it horizontally in the plane of the sensitive area at a rate of about 0.08 inch per minute. A stationary aperture stop, having a circular opening 1/16 inch in diameter, was mounted directly in front of the detector. The detector was irradiated through the aperture stop by radiation from a tungsten lamp.

The thermopile consists of ten receivers, each approximately 2 mm by 5 mm in size, arranged in two columns of five rows each to form a sensitive area 1 cm square. A thermocouple was attached to the back of each receiver, and the ten thermocouples were connected in series to form the thermopile. The scans in the A-A' direction were made across the center of the sensitive area, along the line between the two columns. The scans in the B-B' direction were across the center of the sensitive area along the long axis of the two receivers in the third row. In each case, scans were made with a) the incident radiation chopped at 13 cycles per second and amplified with a synchronous amplifier, and b) with unchopped radiation with a d-c amplifier. Results are shown in figure 1 for the a-c scans, and in figure 2 for the d-c scans.

In figure 1 for the A-A' scans, it can be seen that there are three distinct peaks, with some indication of two others, corresponding to the positions of the five rows of plates. In the B-B' scan, it is apparent that the plate on the right had greater sensitivity than that on the left.

In figure 2, the d-c scans in the B-B' direction are somewhat similar to the equivalent a-c scans; the scans in the A-A' direction show five distinct peaks.

At this same time, Mr. Schneider also measured the spatial sensitivity of the Golay cell in a similar manner. In this case, a Globar-filter arrangement provided the different wavelengths. The results are shown in figures 3 and 4.

Angular Sensitivity

To measure the angular sensitivity of the thermopile, the detector was mounted on a milling head (figure 5) with its sensitive area in a vertical plane and with the two columns of thermocouple receivers vertical, in a position such that the center line of the sensitive area coincided with the vertical axis of the milling head. An image of the exit slit of the monochromator, 3 mm by 3 mm in size, was focused on the center of the sensitive area from a direction normal to it, by means of a 6-inch-diameter spherical mirror having a 49-inch radius of curvature. The cone of rays thus had a half-angle width of about $3\frac{1}{2}°$. The monochromator was adjusted to give a band of radiation centered at 2.2 microns. The response of the detector was recorded as R_n when the axial ray of the incident beam was normal to the sensitive area. The milling head was then rotated to give incident angles of 5, 10, 15, 20, 25, 30, 40, 50, 60, and 70° to the normal, and the response of the detector was recorded at each setting as R_θ, θ being the angle of incidence. The data were normalized by the reading at normal incidence, and plotted as a function of angle of incidence to produce the curve shown in figure 6. Similar measurements were made with a cover plate 0.15 inch in thickness with a 1-cm by 1-cm hole mounted over the sensitive area. The entire procedure was repeated with a band of radiation centered at 8 microns.

The experimental curves are compared in figure 6 with two computed theoretical curves.

The top curve, in which $R_n/R_\theta = 1$ at all angles, would be obtained if the detector were equally sensitive to flux striking it at all angles, and if all of the incident flux struck the sensitive area. The lower curve, in which $R_n/R_\theta = \cos\theta$, would be obtained if the detector were equally sensitive to flux striking it at all angles and were completely filled at normal incidence.

From the experimental curves in figure 6 it can be seen that the sensitivity increases slightly from normal to 20°, then decreases. The increase is undoubtedly due to the fact that as the illuminated area of the detector increases, the more sensitive areas, as shown in figures 1 and 2, become irradiated. The sharp drop in response beginning at about 30° is due to some of the flux being lost; either not admitted through the window or not striking the sensitive area if admitted. The presence of the cover plate increases the rate of fall-off in this range, as might be expected.

Similar tests were made with the detector mounted with the five rows of plates vertical. The results shown in figure 7 are similar to those in figure 6, except that the increase in signal from 0° to 20° was not observed. This is due to the fact that as the angle was increased, more plates were illuminated, but in the same relative areas; hence the signal remained constant.

The curves plotted in figures 6 and 7 show no significant differences for fluxes of 2.2 and 8 microns, respectively. The fact that the curves are nearly flat from 0° to 25° indicates that variation in angular sensitivity will be a problem only when the marginal rays of an incident beam exceed 25°.

APPENDIX B

SPHERE COATINGS

Several types of sphere coatings were prepared for use as described in the body of this paper. This section briefly outlines the methods used in preparation of these surfaces. In each case, two hemispheres were coated and then joined to form the sphere.

Sulfur

All sulfur used in this work was Crystex brand sulfur; however, reference (9) indicates that ordinary flowers of sulfur has about the same reflectance as Crystex brand sulfur throughout the infrared. No effort was made to establish the usefulness of forms of sulfur other than Crystex brand sulfur. It should also be noted that Stauffer Chemical Company also supplies Crystex brand sulfur which contains 20 percent by weight of oil and which has excellent mechanical properties. However, information on the reflectance is not available. Several different techniques were used to apply sulfur to the sphere walls, as follows:

Hand Pressed: Initially, sulfur was applied to the sphere over a thin coat of rubber cement by hand pressing (with the fingers). The sulfur was built up to a thickness of about 1/8 inch, and contoured to roughly conform to the outline of the two hemispheres. The surface was then smoothed with an artist's brush. This surface had a fairly uniform appearance, but the coating was extremely fragile.

Sulfur-Alcohol Slurry: To increase the uniformity of the coating over the surface of the sphere and the reproducibility from one sphere to another, a spray application technique was investigated. One part sulfur was mixed with about two parts alcohol by volume to form a slurry which was sprayed from a vibrator-activated spray gun. The slurry was sprayed so that most of the alcohol evaporated before the spray hit the roughened (approximately 50μ in. rms) sphere wall. To insure rapid evaporation of the remaining alcohol, the hemispheres were heated to 170° F before spraying. About ten spray applications were necessary to obtain a 1/8-inch coating. The hemispheres were reheated to 170° F and the sulfur surface was smoothed with an artist's brush between application. The resulting coating was very uniform in appearance, but it tended to crack with time and its adherence to the metal hemisphere was poor. The sulfur itself formed a comparatively hard surface.

Benzene-Sulfur Slurry: To alleviate the problems experienced with the sulfur-alcohol slurry, the alcohol was replaced by benzene. This slurry was applied to the roughened hemisphere wall over a thin coat of a benzene-soluble contact cement. During the first few seconds of spraying, the spray gun was held very close to the surface so that the benzene dissolved the contact cement, which migrated slightly into the sulfur coating. The thin coating was then dried, leaving the sulfur bonded to the sphere wall. For the subsequent spraying operation, the spray gun was moved further away from the sphere wall, the temperature of which was maintained at about 150° F by heat from two infrared lamps. This, and the fact that benzene is more volatile than alcohol, permitted the slurry to be sprayed continuously until a coating thickness of about 1/8 inch was obtained. The surface was then smoothed with an artist's brush. The surface produced by this technique was very uniform in appearance and mechanically strong enough to withstand normal laboratory handling. The surface hardened considerably with age.

$BaSO_4$ Surfaces

A $BaSO_4$-benzene slurry was sprayed in the same manner as the sulfur-benzene slurry to coat spheres with $BaSO_4$.

Gold-Roughened Surfaces

Several spheres were roughened with glass and steel spherical shot by the Pangborn

Corp., using a Roto-Blast process. The glass shot (Pangborn No. L) are -200+325 mesh SAE and yield a surface roughness on the aluminum sphere of about 25μ in. rms. The steel shot (Pangborn No. S-460) are 10 mesh SAE and yield a surface roughness on the aluminum spheres of about 150μ in. rms. After the hemispheres had been uniformly roughened with one of the above shots, they were cleaned and gold was vapor-deposited onto the surface.

Certain commercial materials are identified in this paper in order to adequately specify the materials employed. In no case does such identification imply that the material identified is necessarily the best available for the purpose.

REFERENCES

(1) a. Stair, R. and Schneider, W. E., "Standards, Sources, and Detectors in Radiation Measurements." Symposium on Thermal Radiation of Solids. Editor: Dr. Samuel Katzoff. NASA SP-55. To be published in 1965.

b. Stair, R.; Schneider, W. E.; Water, W. R.; and Jackson, J. K., "Some Factors Affecting the Sensitivity and Spectral Response of Thermoelectric (Radiometric) Detectors, Applied Optics V. 4, No. 6, June 1965, pages 703-710.

c. Coblentz, W. W., "The Radiation Sensitivity as a Function of Area Exposed." Bulletin of the Bureau of Standards, V. 11, 1915, page 142.

(2) Dunn, S. T., "Design and Analysis of Ellipsoidal Mirror Reflectometer." Ph.D. Thesis, Oklahoma State University, May, 1965.

(3) Stair, R.; Schneider, W. E.; Waters, W. R.; Jackson, J. J.; and Brown, R. E., "Some Developments in Improved Methods for the Measurement of the Spectral Irradiances of Solar Simulators." NASA Contract Report CR-201, April, 1965.

(4) Bennett, H. E. and Koehler, W. F., "Precision Measurement of Absolute Specular Reflectance with Minimized Systematic Errors." Journal of the Optical Society of America, V. 50, 1960, pages 1-6.

(5) Ronzhin, V. V., "A Photomultiplier for Measuring Radiant Flux in Lighted Models with an Absorbing Medium." Iz vestis Vysshikh Uchebnykh Zavedeniy, Priborostroyeniye, No. 1, 1961, pages 94-98.

(6) Richmond, J. C.; Dunn, S. T.; DeWitt, D. P.; and Hayes, W. D., "Procedures for Precise Measurement of Thermal Radiation Properties." November, 1963 - October, 1964, National Bureau of Standards Technical Note to be published in 1965.

(7) Jacques, J. A. and Kuppenheim, H. F., "Theory of the Integrating Sphere." Journal of the Optical Society of America, V. 45, 1955, pages 460-470.

(8) Birkebak, R. C., "Monochromatic Directional Distribution of Reflected Thermal Radiation from Roughened Surfaces." Ph.D. Thesis, University of Minnesota, 1962.

(9) Kronstein, M.; Kraushaas, R. J. and Deacle, R. E., "Sulfur as a Standard of Reflectance in the Infrared." Journal of the Optical Society of America, V. 53, 1963, pages 458-465.

(10) Agnew, J. T. and McQuistan, R. B., "Experiments Concerning Infrared Diffuse Reflectance Standards in the Range .8 to 20.0 Microns." Journal of the Optical Society of America, V. 43, 1953, pages 999-1007.

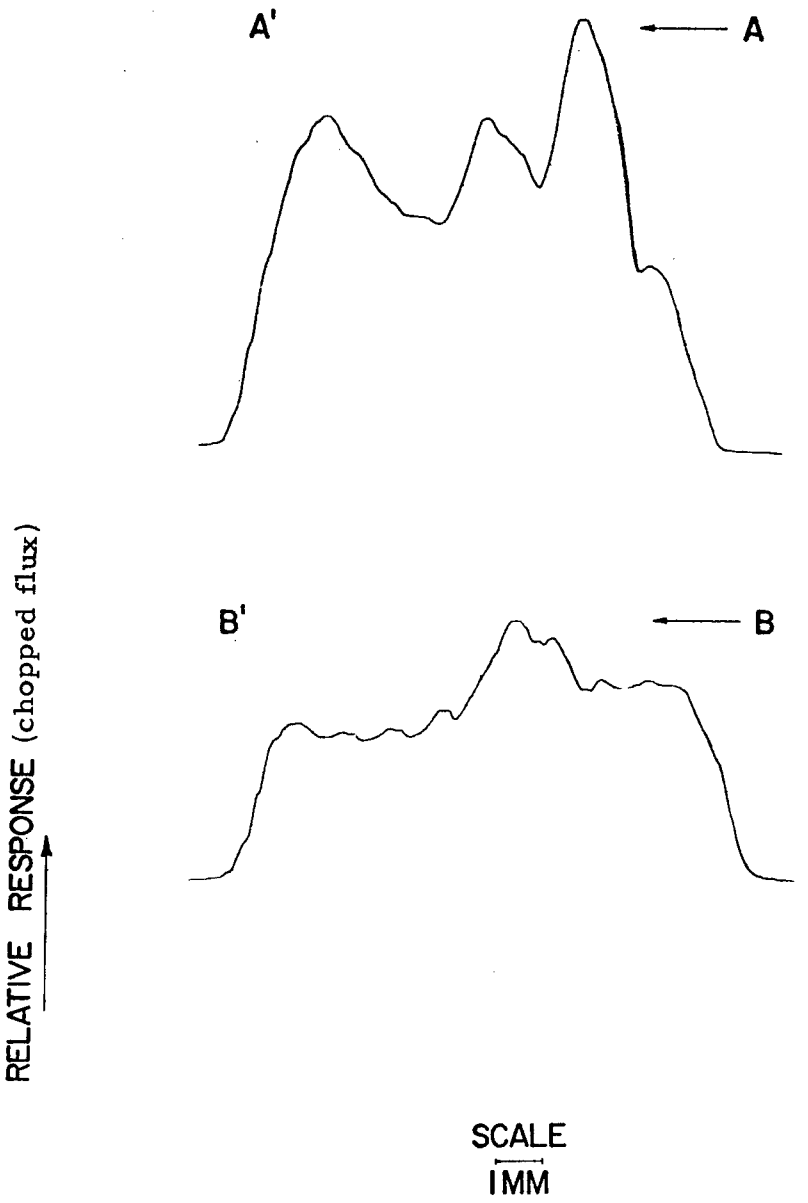

Results of Scans Across the Sensitive Area of the Thermopile Detector in the A-A' and B-B' Directions, With Chopped Tungsten Incident Flux.

The A-A' direction is across five rows of plates, and the B-B' direction is across two columns of plates.

Figure 1

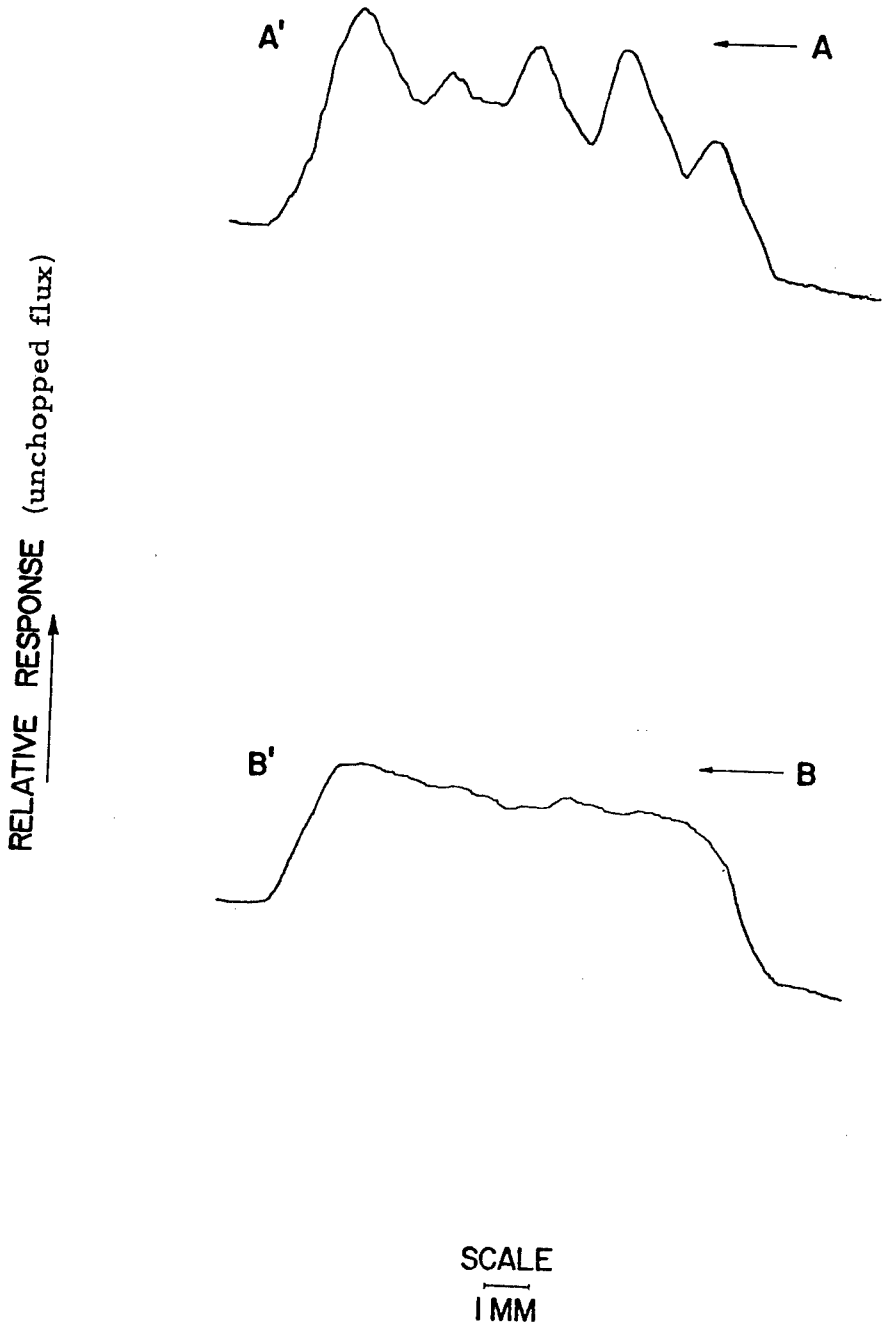

Results of Scans Across the Sensitive Area of the Thermopile Detector in the A-A' and B-B' Directions, With Unchopped Tungsten Incident Flux.

The A-A' direction is across five rows of plates, and the B-B' direction is across two columns of plates.

Figure 2

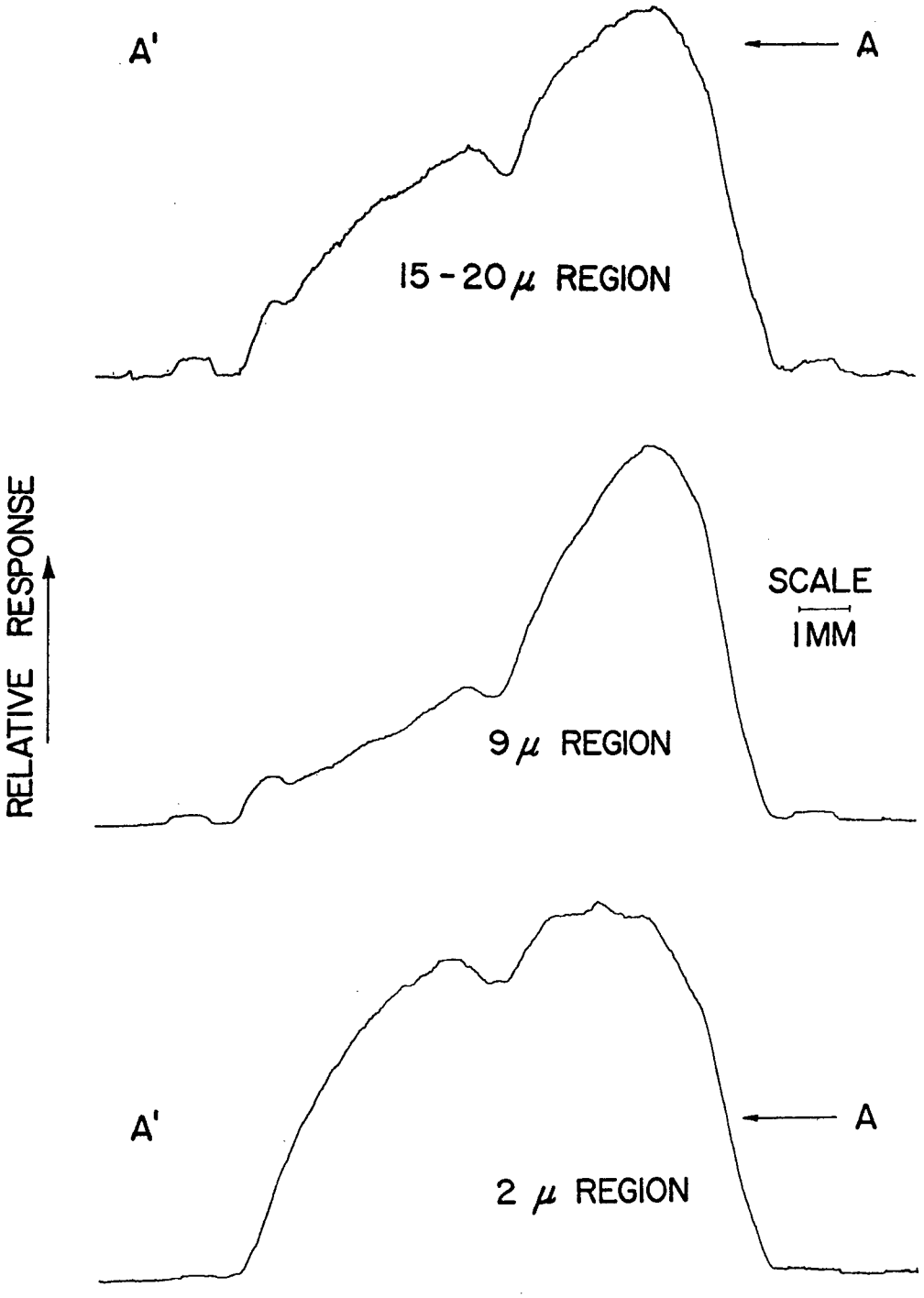

Results of Scan Across the Sensitive Area of the Golay Cell Detector in the A-A' Direction, With Incident Flux in Three Different Wavelength Regions as Indicated.

Figure 3

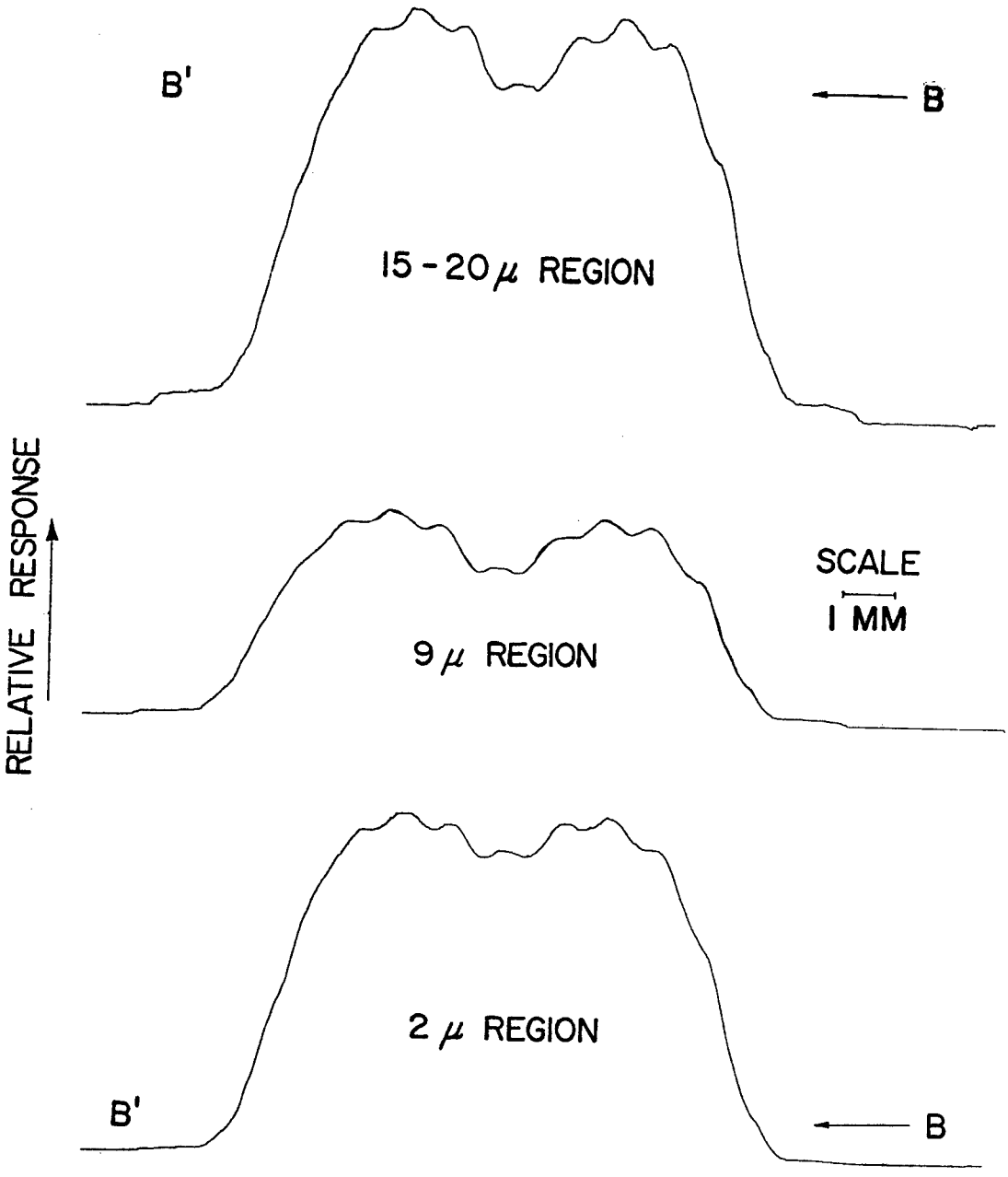

Results of Scan Across the Sensitive Area of the Golay Cell Detector in the B-B' Direction, With Incident Flux in Three Different Wavelength Regions as Indicated. (The B-B' is perpendicular to the arbitrary A-A' direction.)

Figure 4

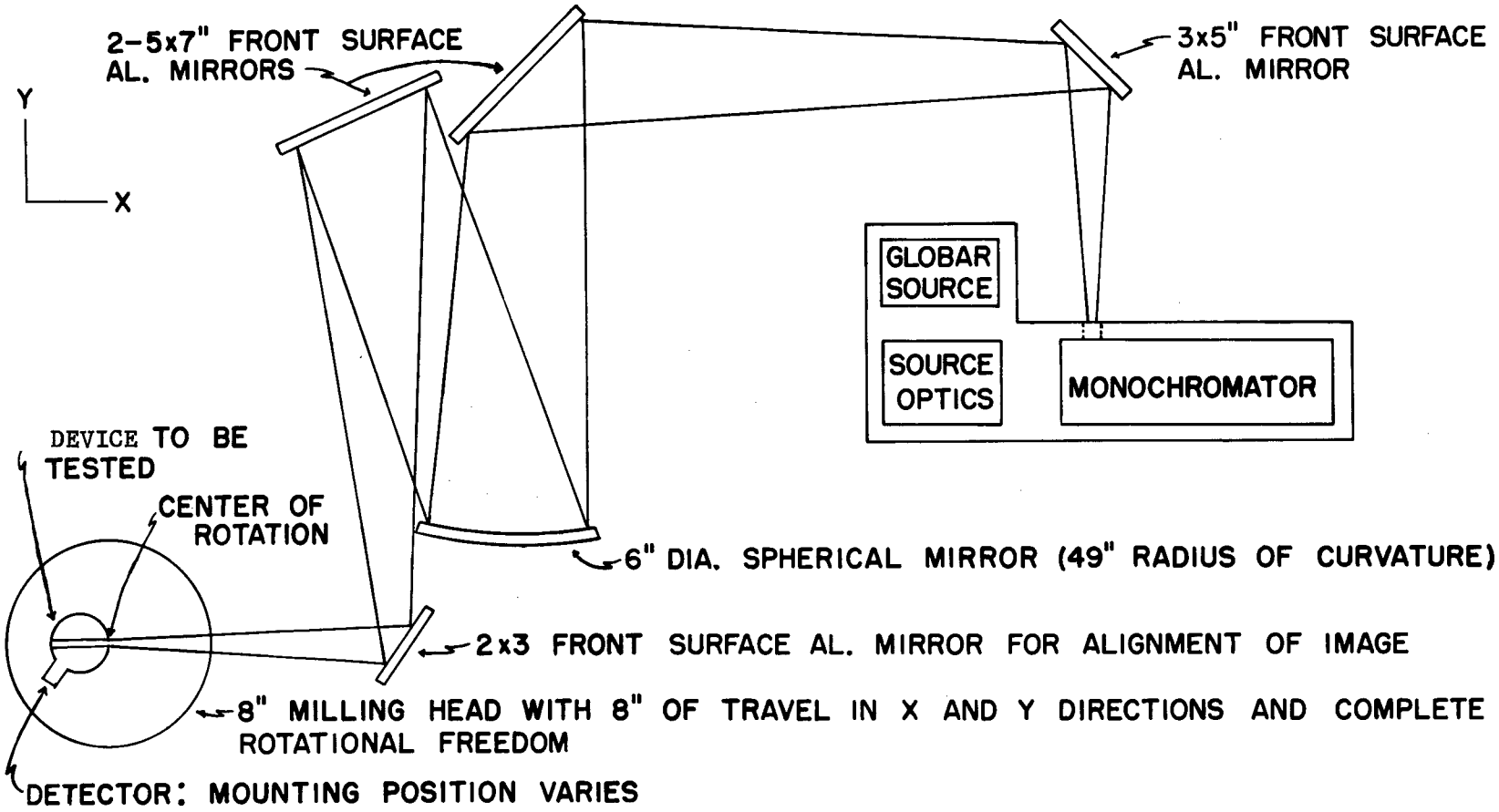

Spatial and Angular Sensitivity Test Apparatus

Figure 5

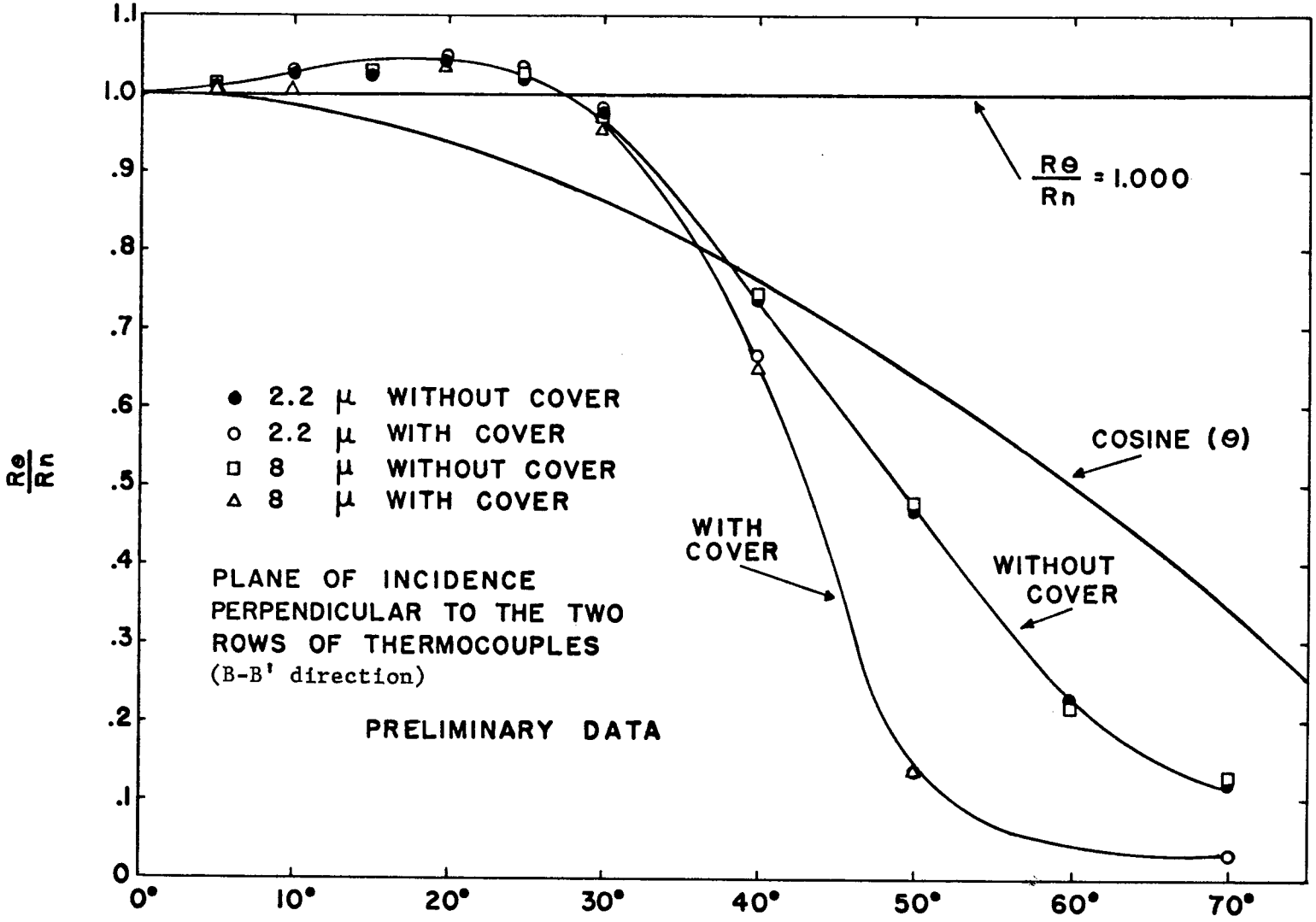

Angular Sensitivity of Reeder Thermopile Across the Two Rows of Thermocouples

Figure 6

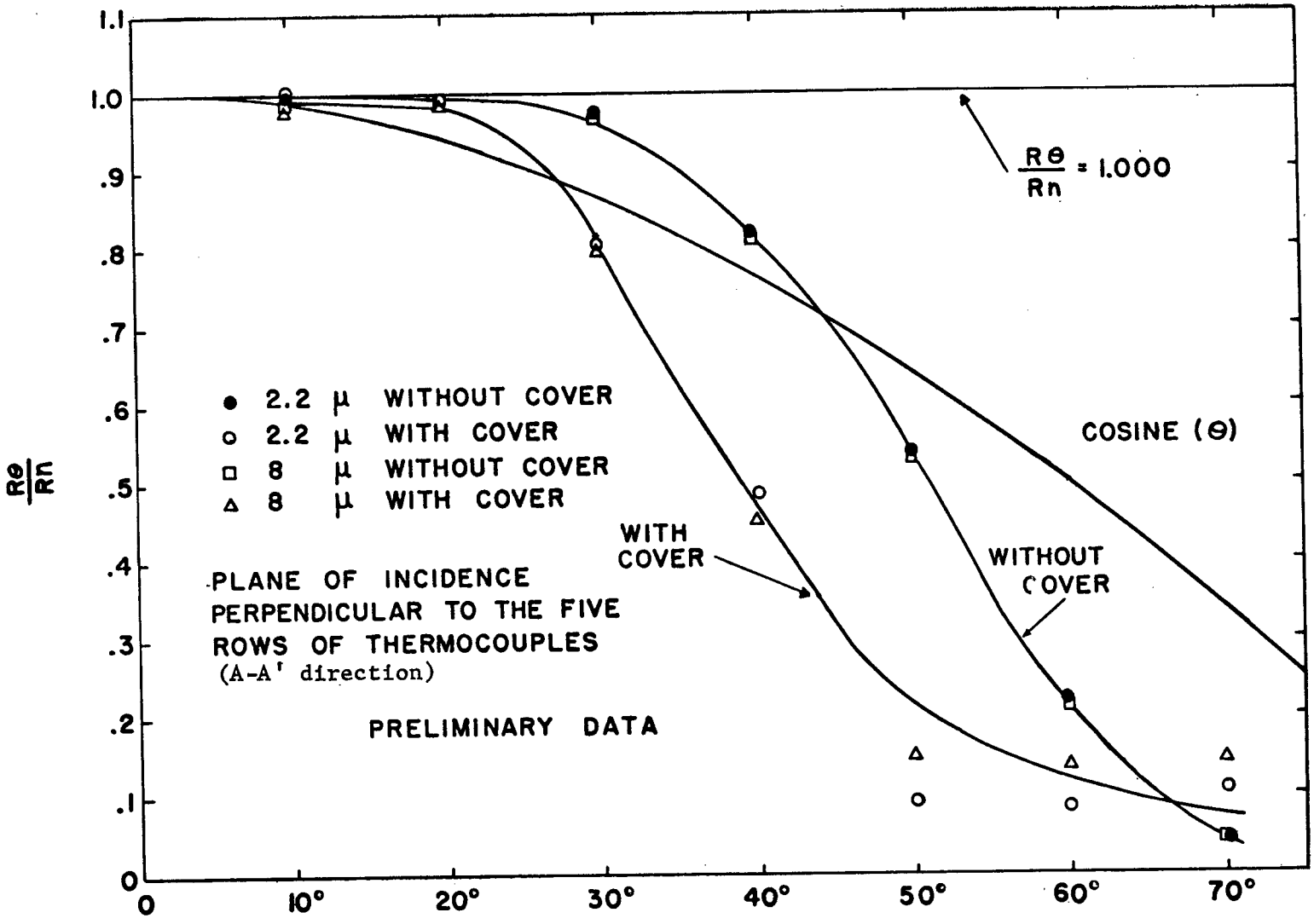

Angular Sensitivity of Reeder Thermopile Across the Five Rows of Thermocouples

Figure 7

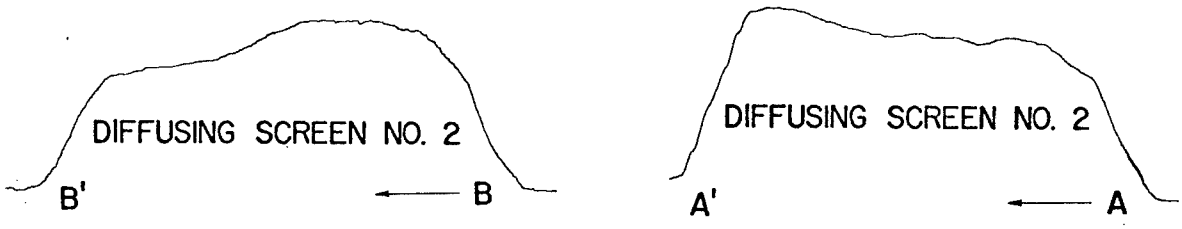

Results of scans across the sensitive area of the thermopile detector in the A-A' and B-B' directions, with unchopped tungsten incident flux. The A-A' direction is across five rows of plates, and the B-B' direction is across two columns of plates.

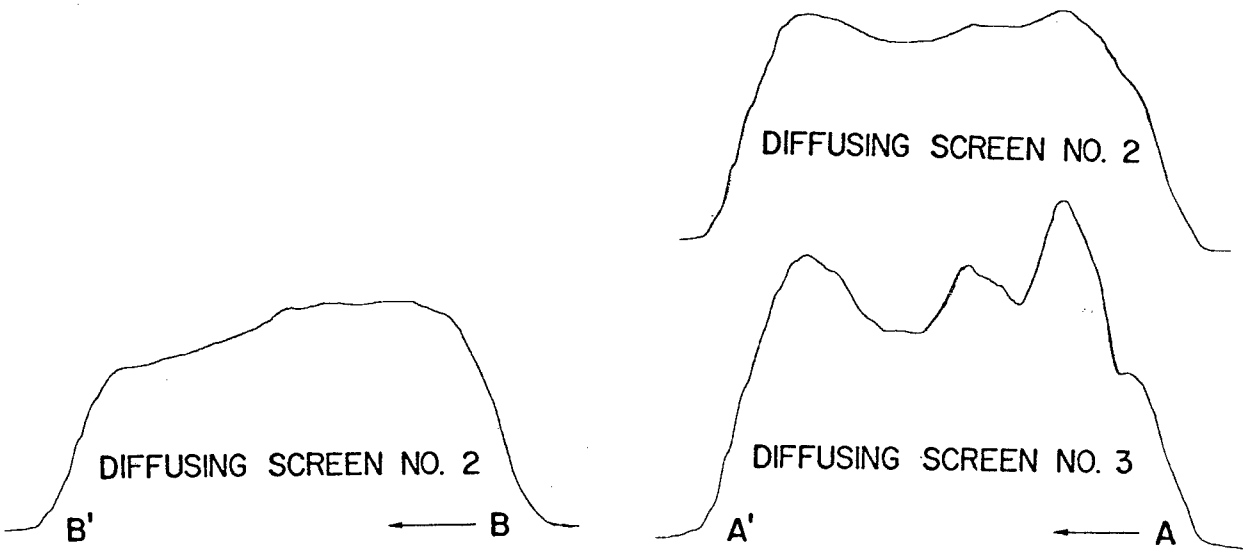

Results of scans across the sensitive area of the thermopile detector in the A-A' and B-B' directions, with chopped tungsten incident flux. The A-A' direction is across five rows of plates, and the B-B' direction is across two columns of plates.

Results of Spatial Sensitivity Test for NaCl Diffusing Screen
(Reprinted from reference 6)

Figure 8

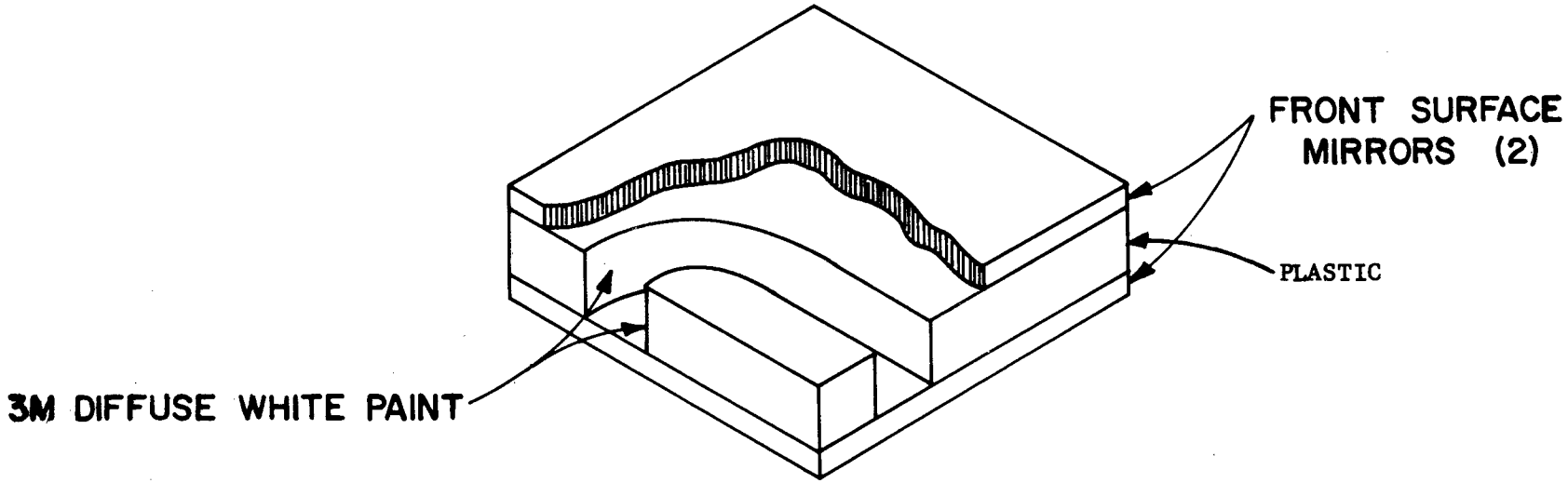

Diffusing Elbow

Figure 9

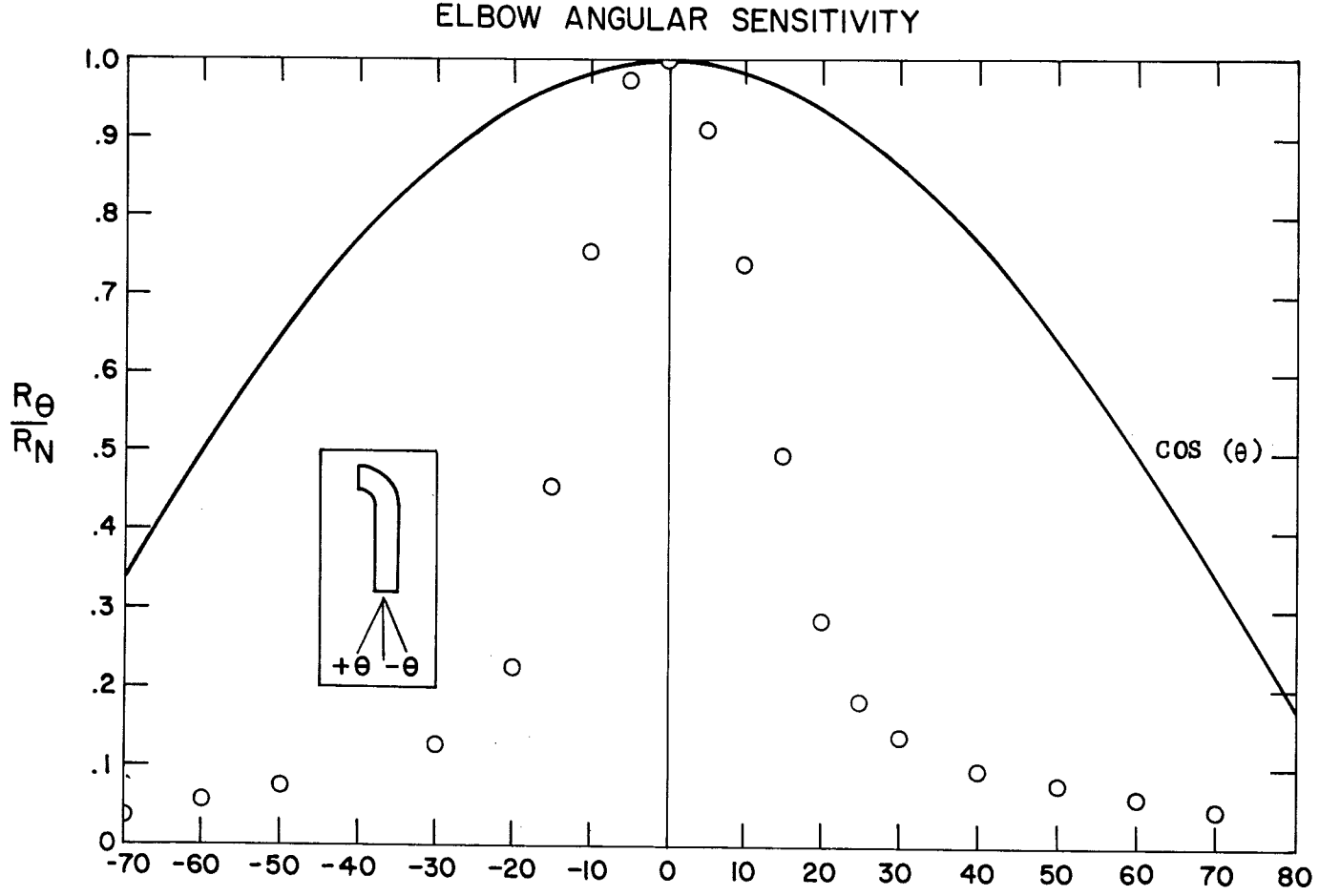

Angular Sensitivity of Diffusing Elbow

Figure 10

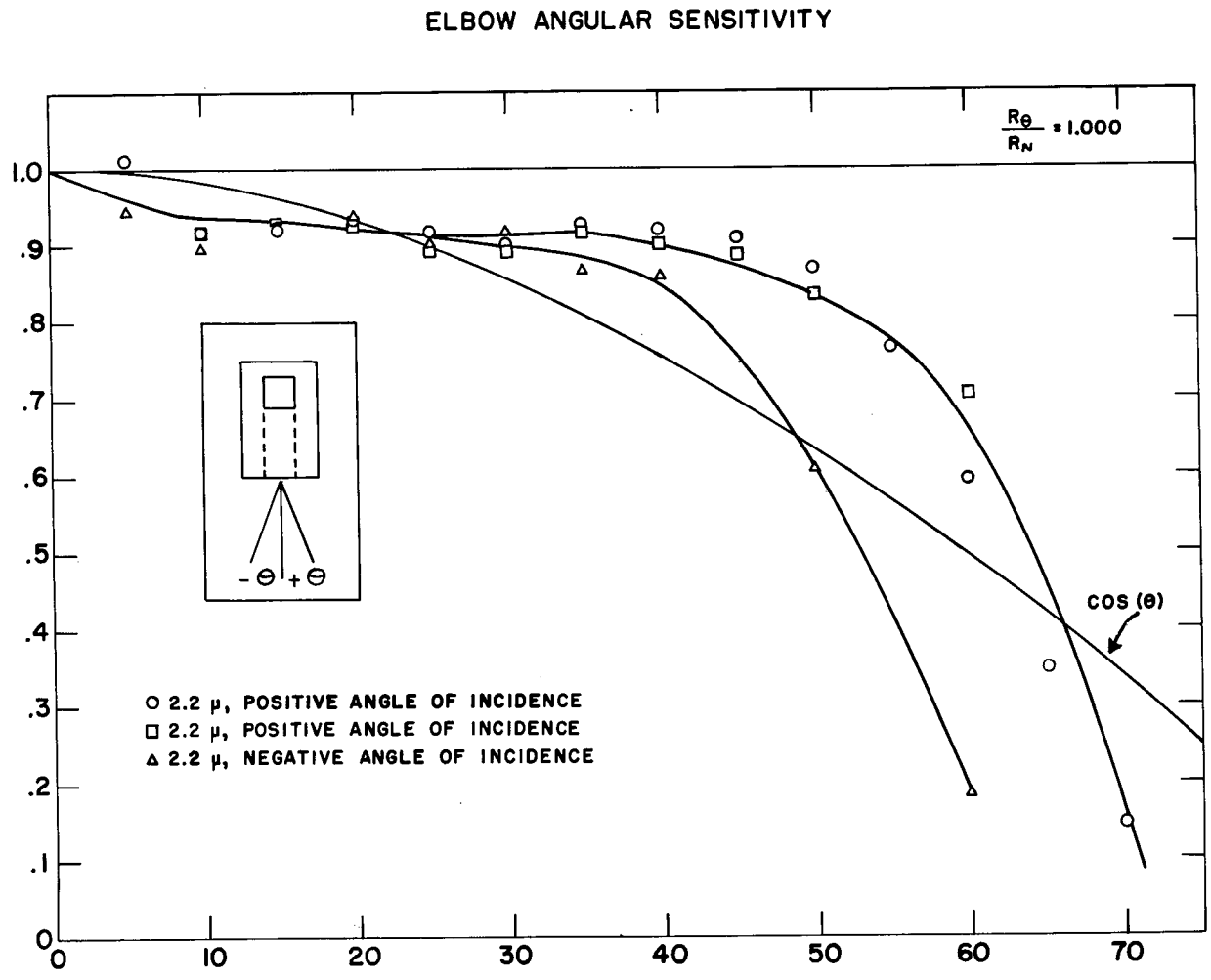

Angular Sensitivity of Diffusing Elbow (B)

Figure 11

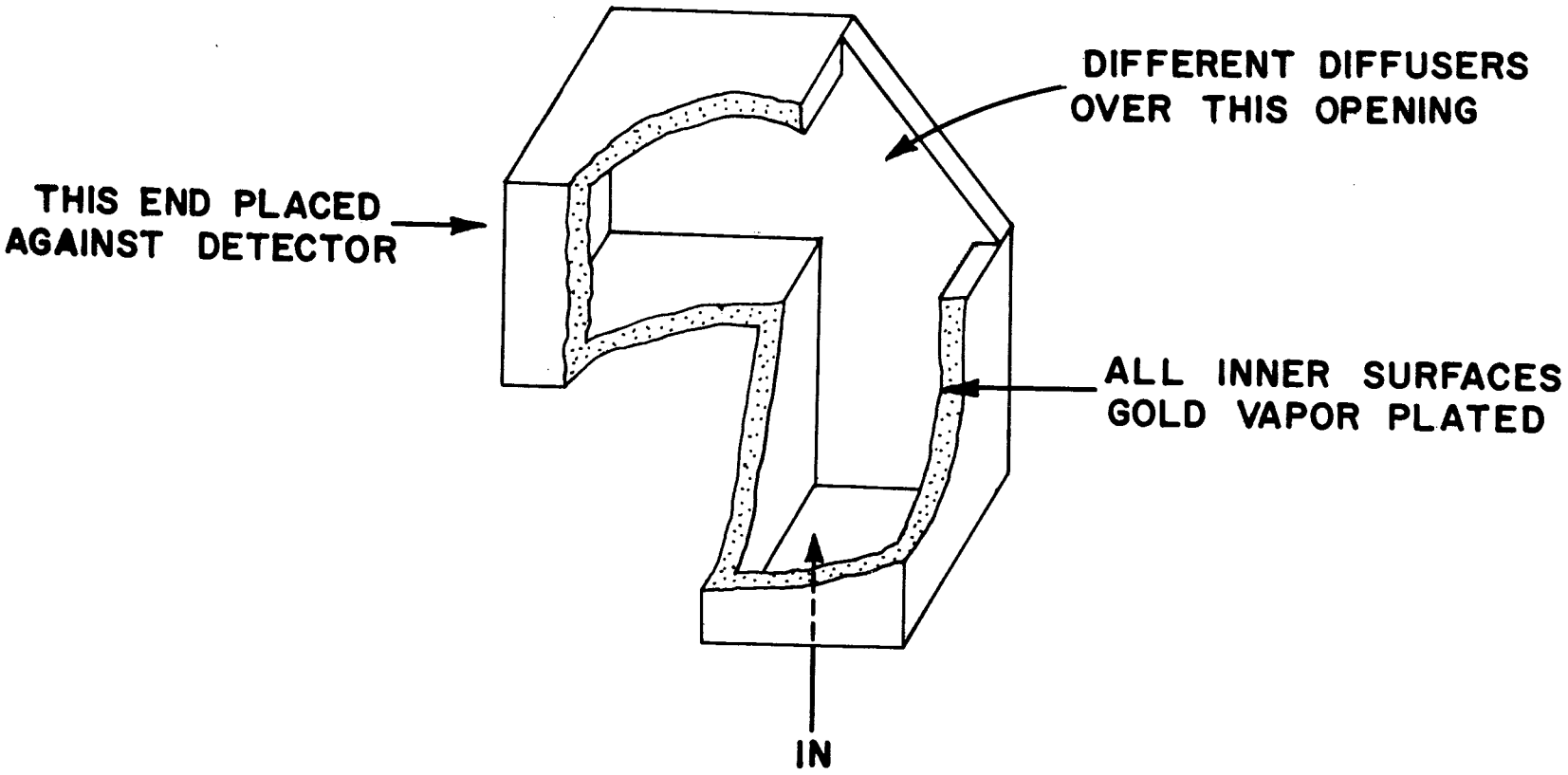

45° Diffusing Elbow

Figure 12

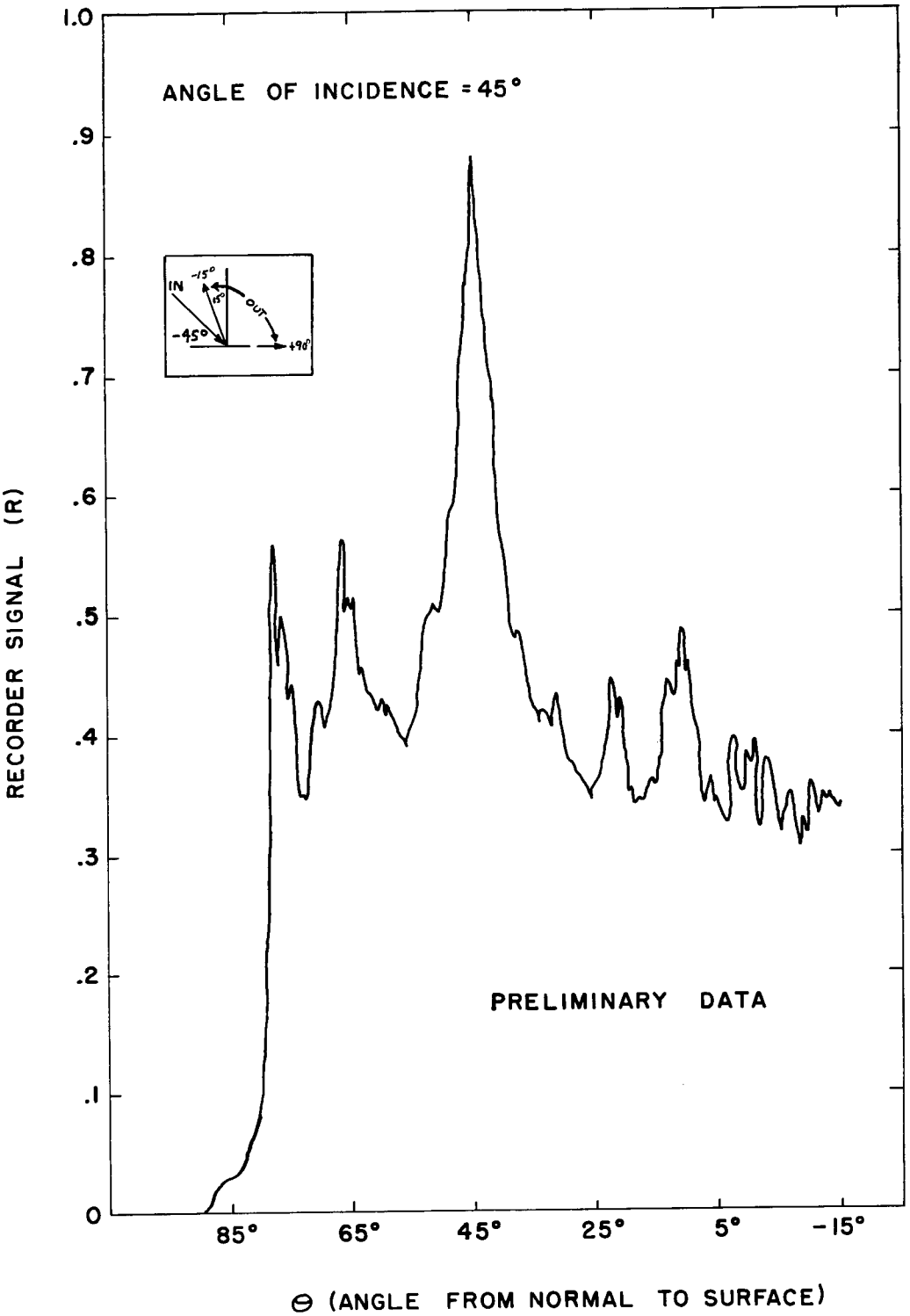

Goniophotometric Data of Spherical Impression Surface

Figure 13

(Taken by Dave Goebel, Photometry & Colorimetry Section, Metrology Division, Institute for Basic Standards, National Bureau of Standards)

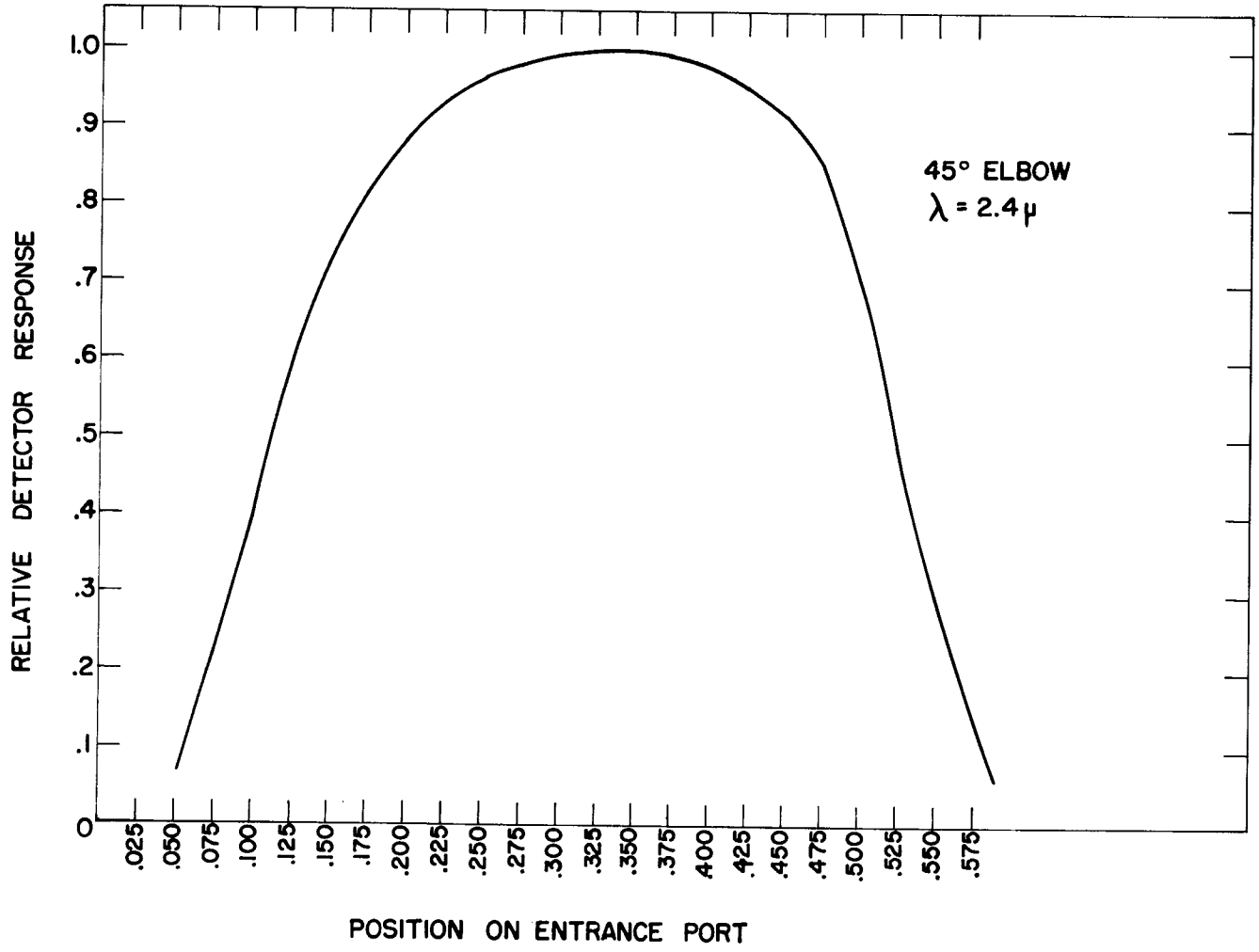

Spatial Sensitivity of 45° Diffusing Elbow

Figure 14

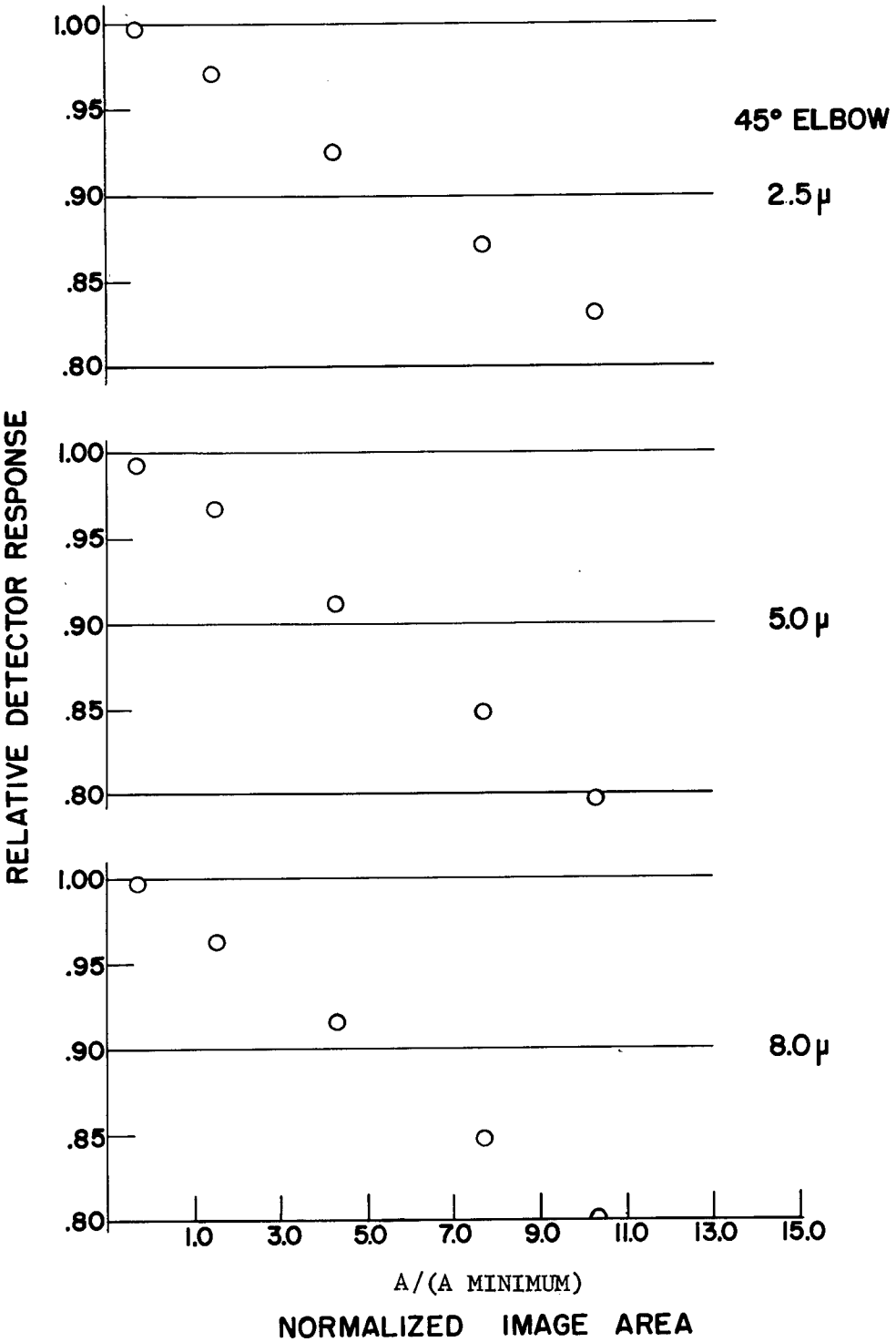

Area Sensitivity Test of 45° Diffusing Elbow

Figure 15

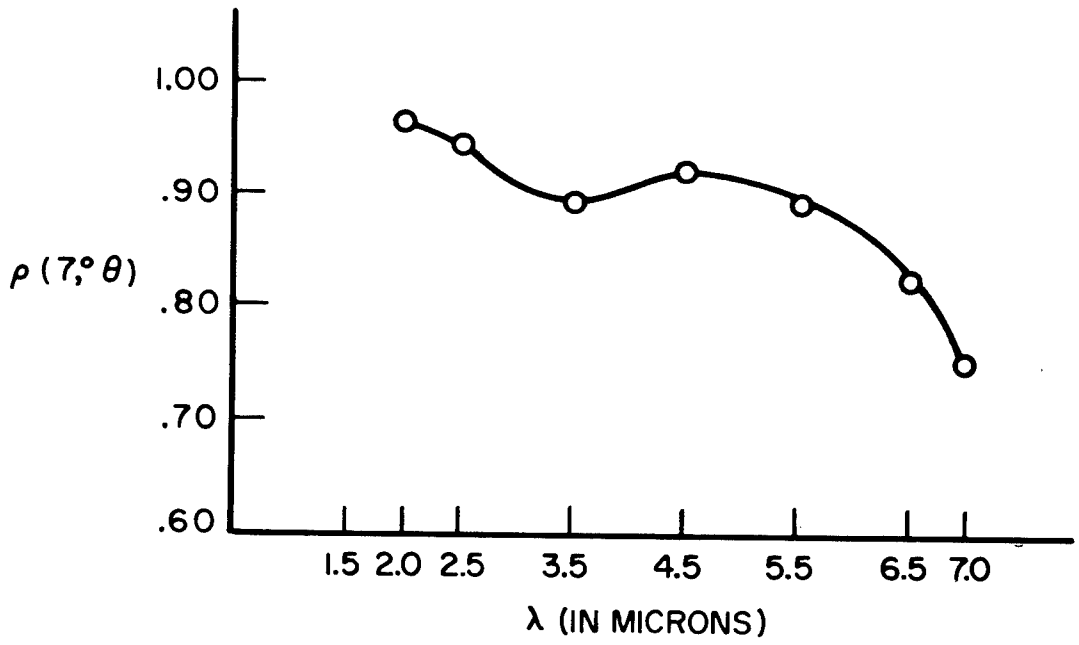

Reflectance of Crystex Sulfur

Figure 16

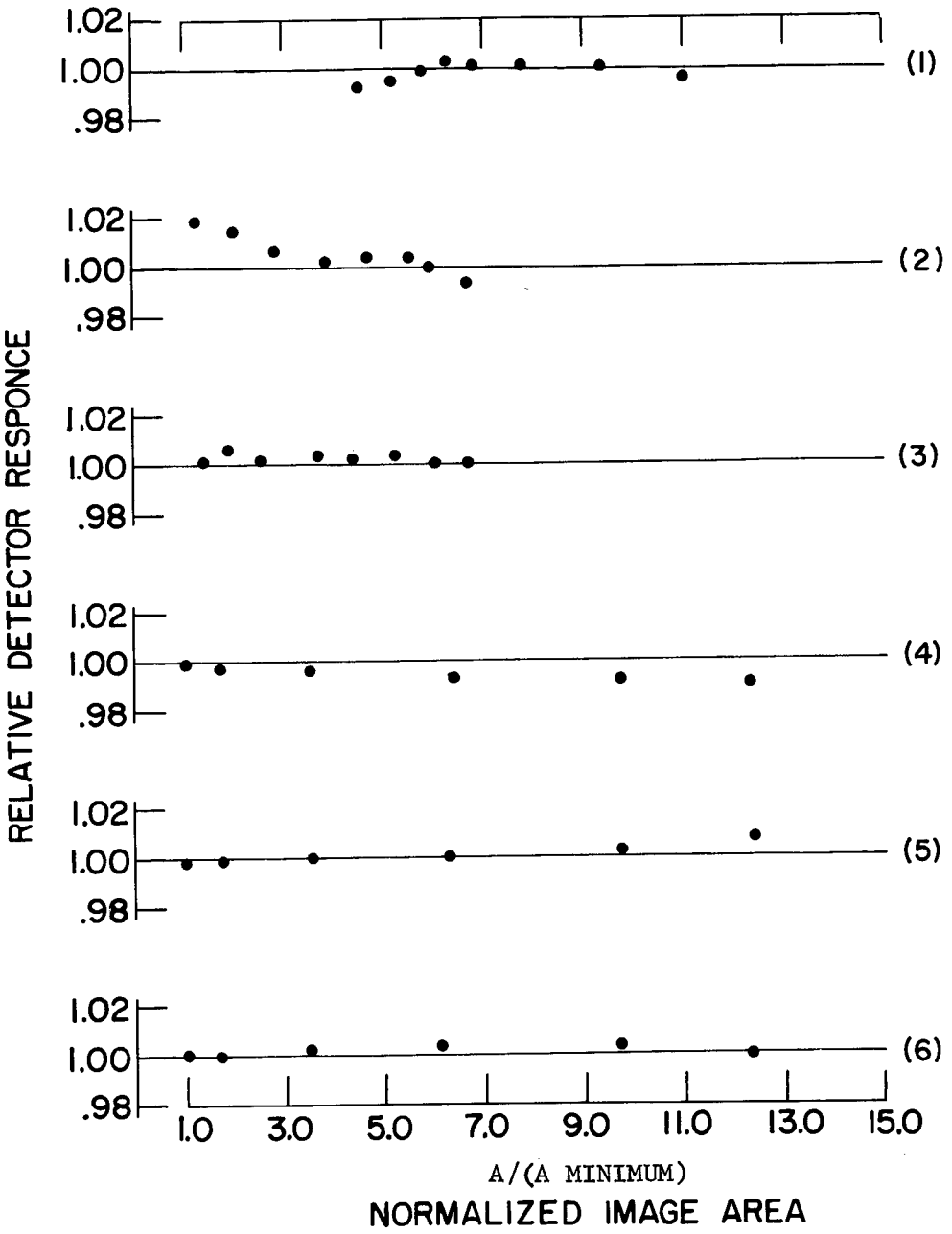

(1) 4" MgO SPHERE a 1.5μ
(2) 2" L-SHOT GOLD SPHERE a 2.4μ
(3) 2" HAND PRESSED SULFUR SPHERE a 2.4μ
(4) 2" GOLD SULFUR SPHERE a 2.4μ
(5) 2" SULFUR SPHERE a 2.4μ SHIELD #1
(6) 2" SULFUR SPHERE a 2.4μ SHIELD #2

Results of Area Sensitivity Test for Various Sphere Coatings

Figure 17

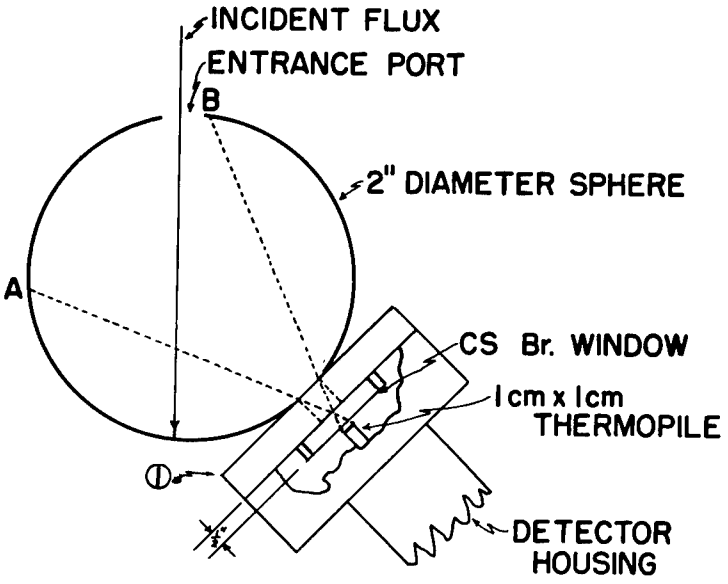

A-B IS FIELD OF VIEW FOR THE DETECTOR

① BLACKENED .15" SHIELD

a) EXTERNAL SHIELD

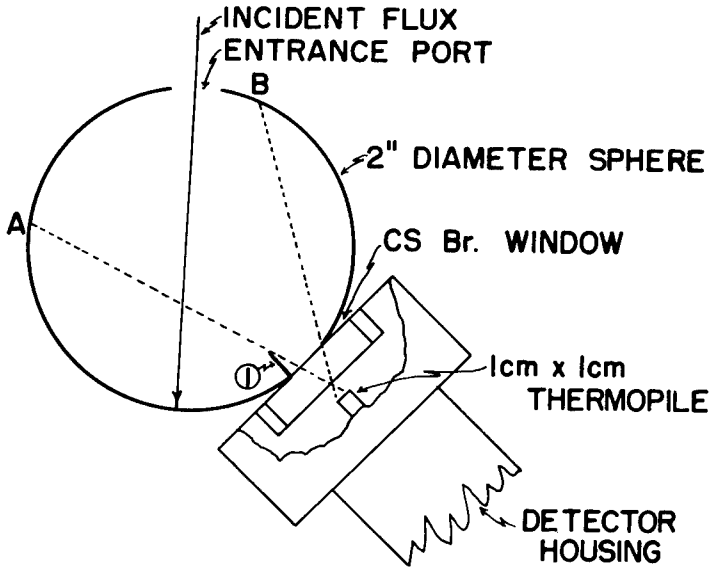

A-B IS FIELD OF VIEW FOR THE DETECTOR

① POLISHED PLATINUM SHIELD

b) INTERNAL SHIELD

Shield Configurations for Averaging Spheres

Figure 18

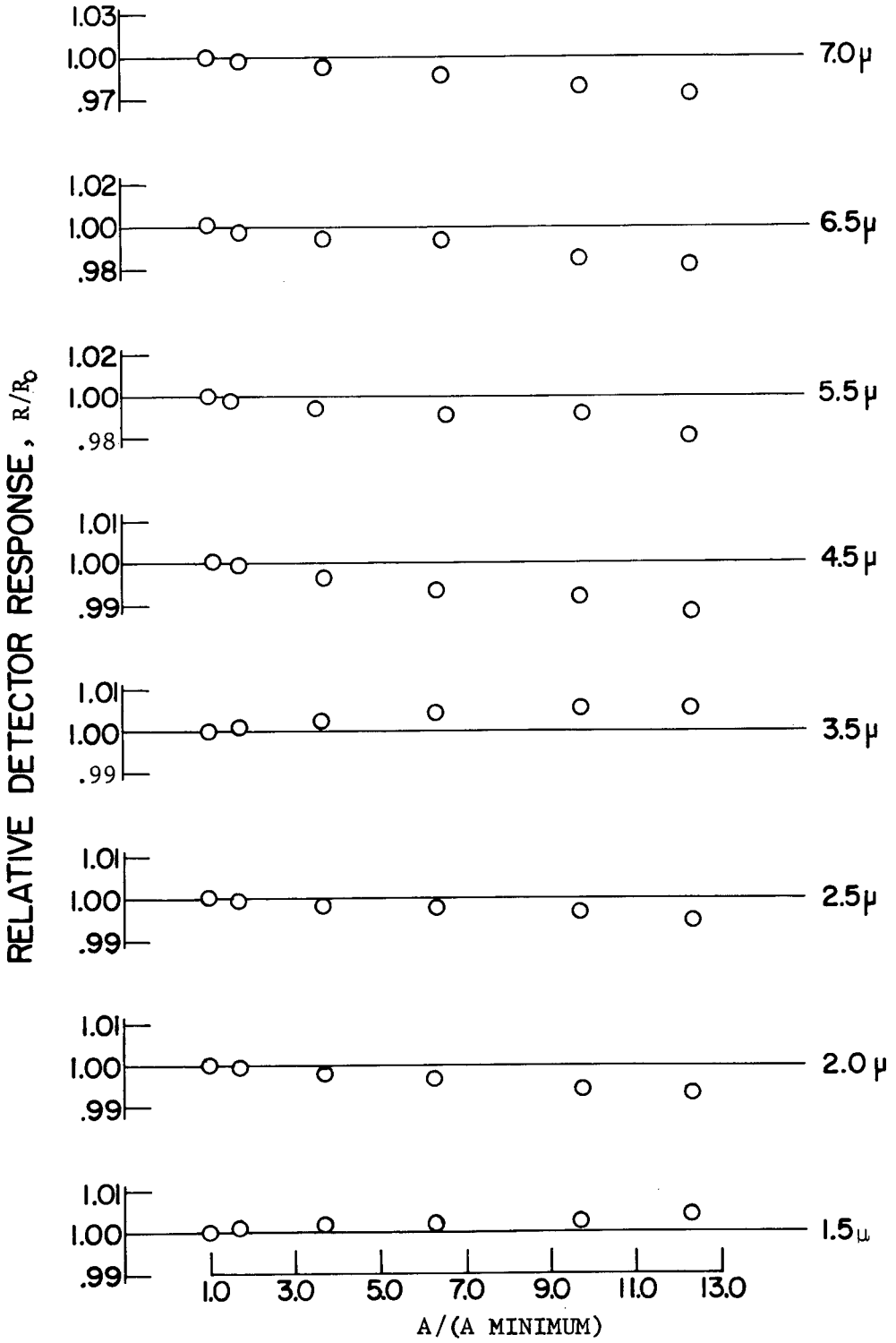

Area Sensitivity Test Results for Internal Shield With the Sulfur-Coated Sphere

Figure 19

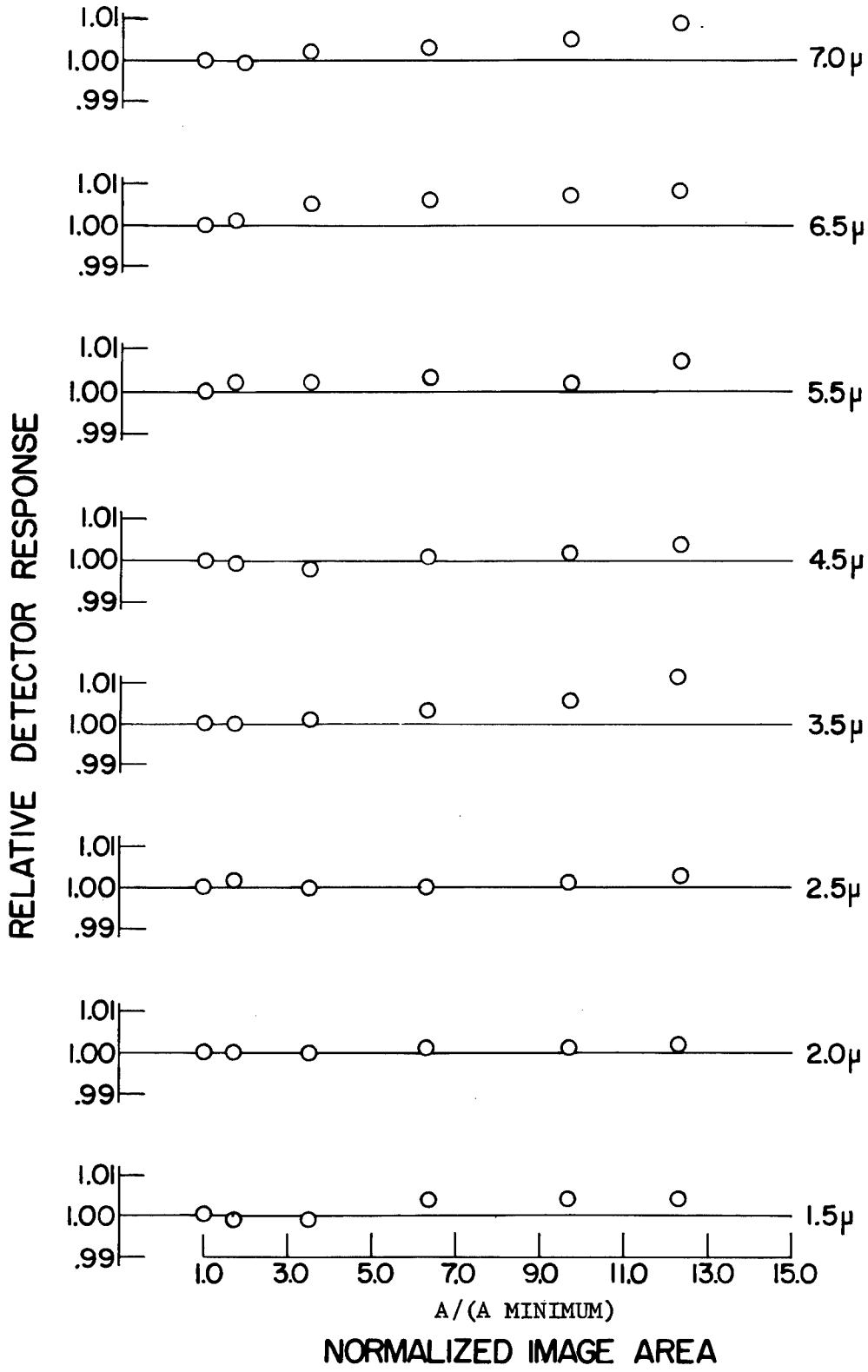

Results of Area Sensitivity Test of Sulfur-Coated Sphere With External Shield

Figure 20

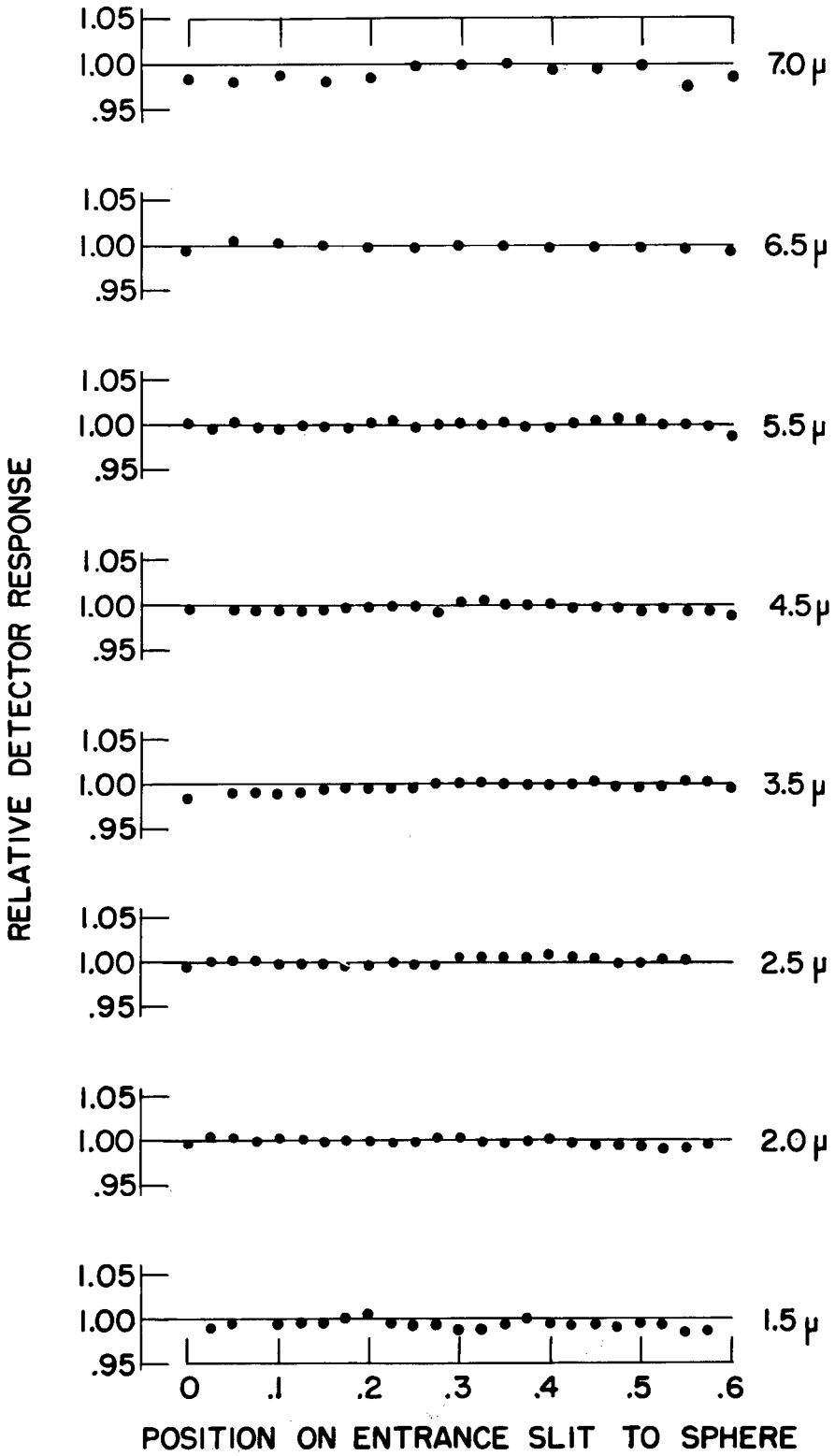

Results of Spatial Sensitivity Test of Sulfur-Coated Sphere With the Internal Shield

Figure 21

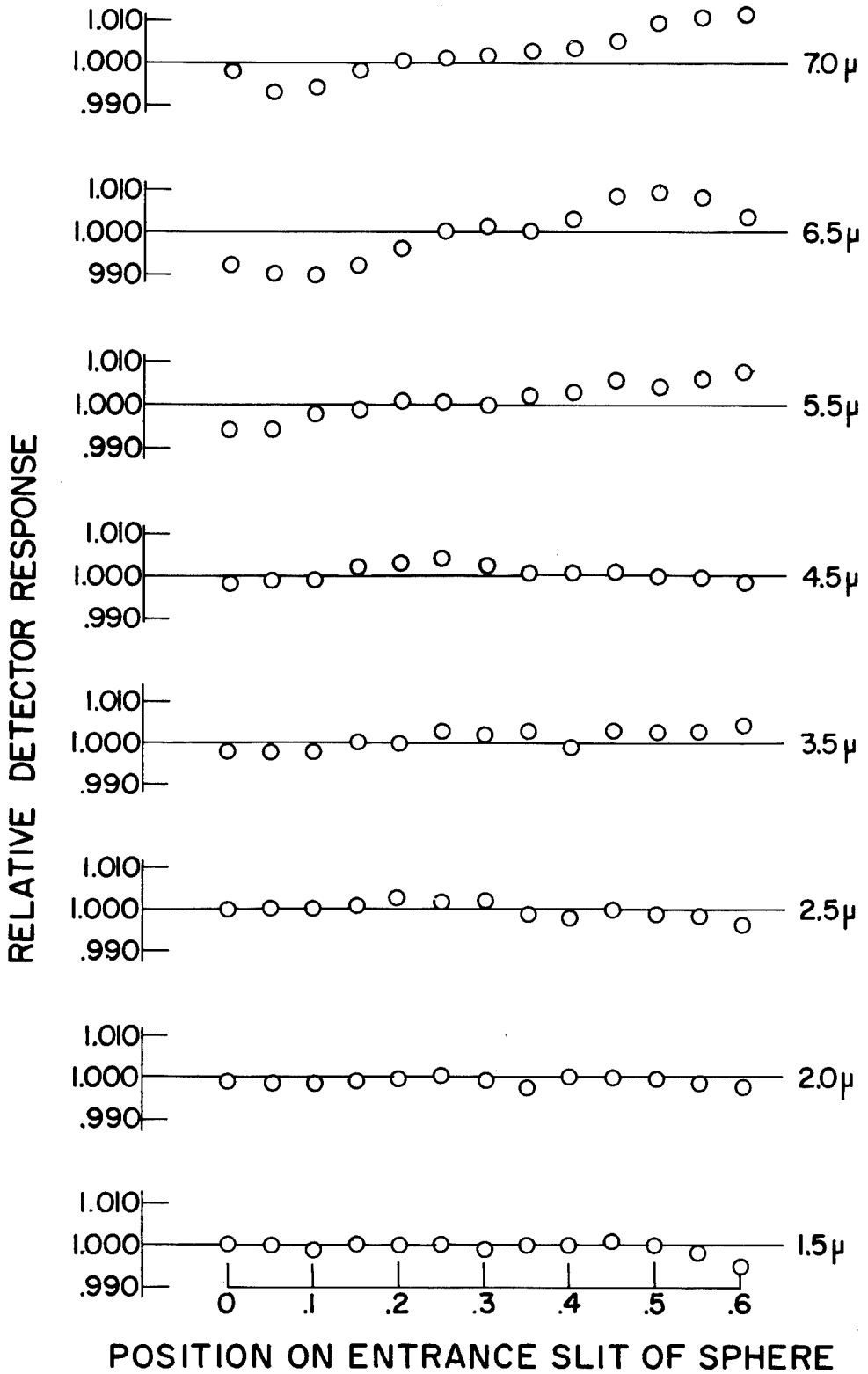

Results of Spatial Sensitivity Test for the Sulfur-Coated Sphere With the External Shield

Figure 22

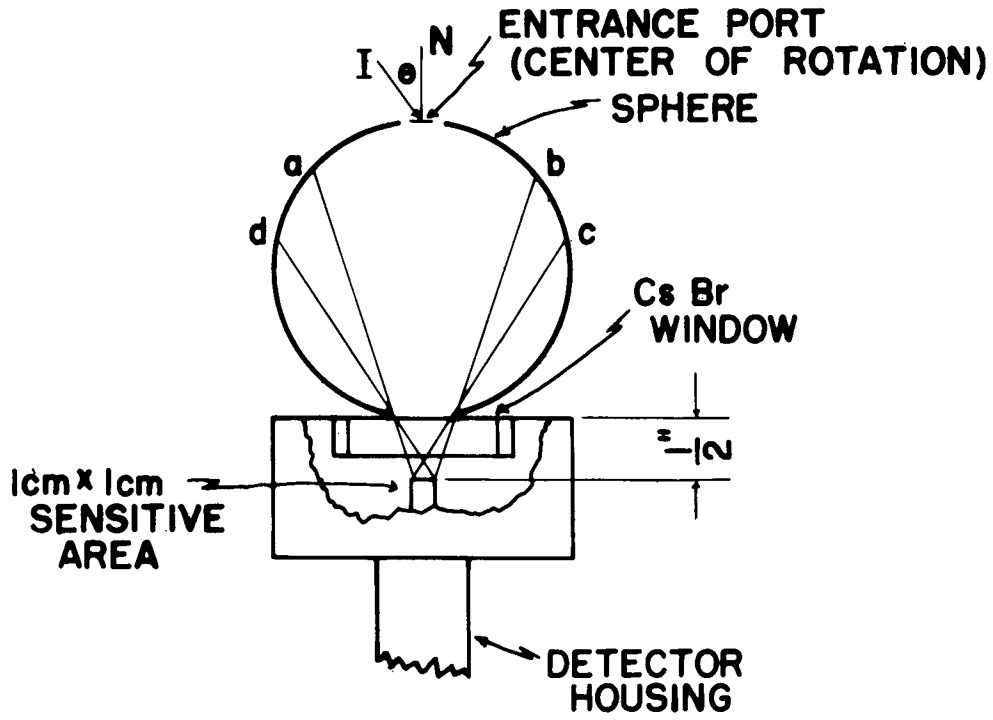

GENERAL DETECTOR VIEWING CONFIGURATION

Model for Sphere Angular Sensitivity Test

Figure 23

S-460 SHOT GOLD PLATED SPHERE (2" DIAMETER)

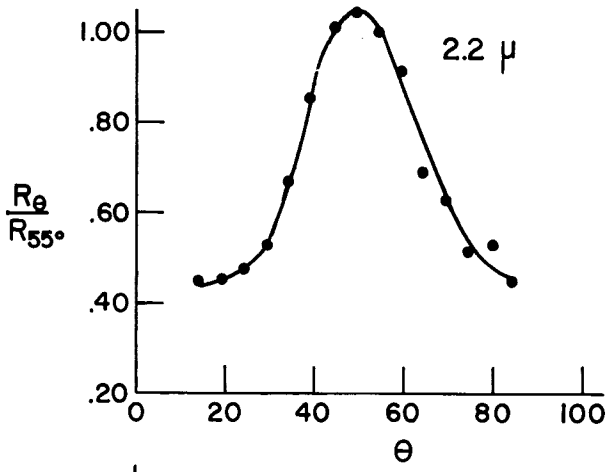

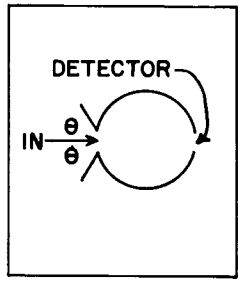

θ IS THE ANGLE OF INCIDENT BEAM MEASURED FROM THE NORMAL TO SPHERE ENTRANCE (in degrees)

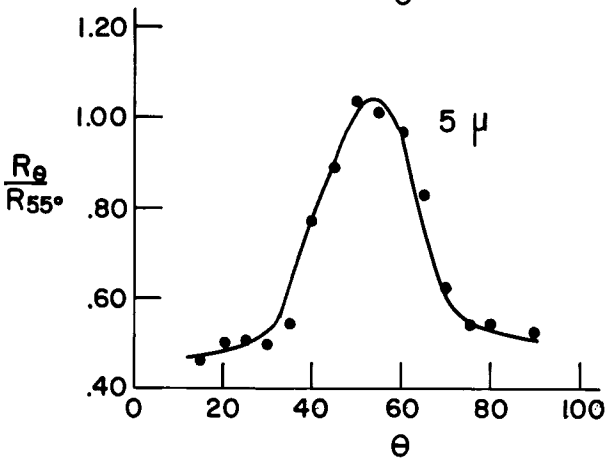

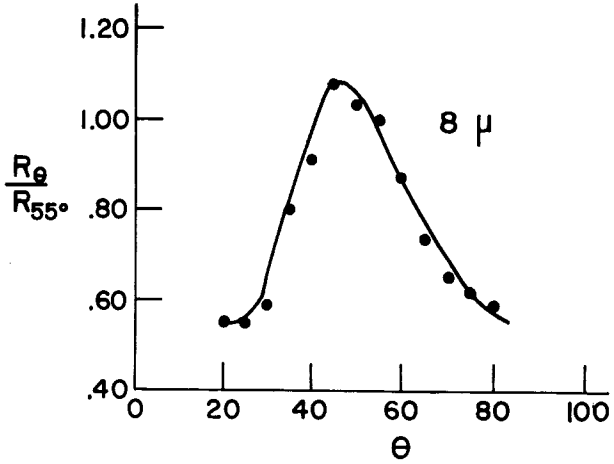

Sphere Test for Gold-Roughened Sphere

Figure 24

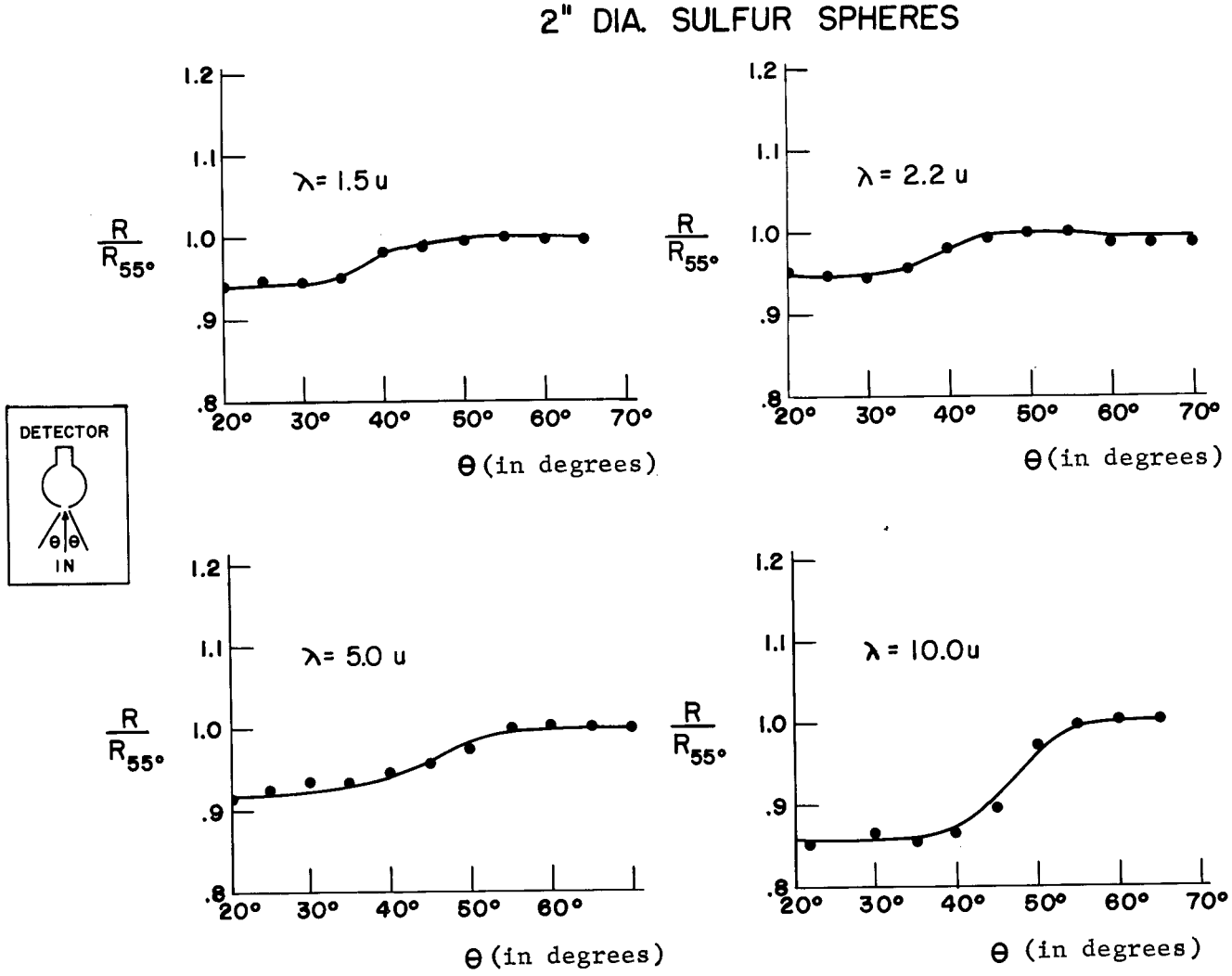

Sphere Test for Sulfur-Coated Sphere

Figure 25